

Impact of Scaffold Exploration on Novel Dual-Acting Histone Deacetylases and Phosphodiesterase 5 Inhibitors for the Treatment of Alzheimer's Disease

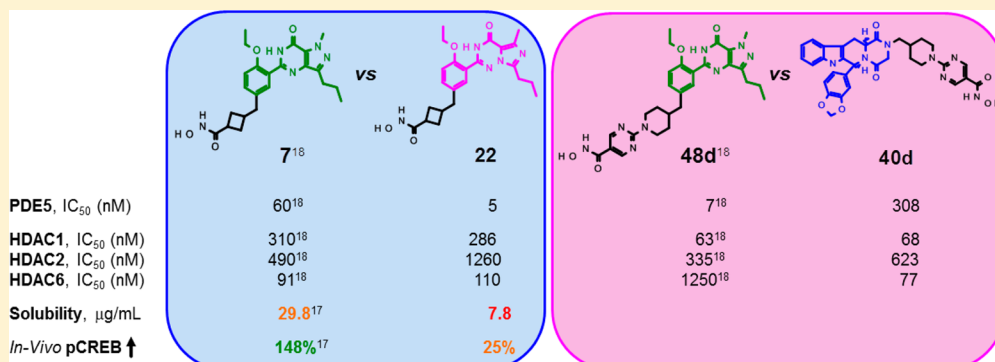
Juan A. Sánchez-Arias,^{†,‡} Obdulia Rabal,^{†,‡} Mar Cuadrado-Tejedor,^{‡,§,⊥} Irene de Miguel,[†] Marta Pérez-González,[‡] Ana Ugarte,[†] Elena Sáez,[†] María Espelosin,[‡] Susana Ursua,[‡] Tan Haizhong,^{||} Wu Wei,^{||} Xu Musheng,^{||} Ana García-Osta,^{†,‡} and Julen Oyarzabal^{*,†,‡,⊥,¶}

[†]Small Molecule Discovery Platform, Molecular Therapeutics Program and [‡]Neurobiology of Alzheimer's disease, Neurosciences Division, Center for Applied Medical Research (CIMA) University of Navarra, Avenida Pio XII 55, E-31008 Pamplona, Spain

[§]Anatomy Department, School of Medicine, University of Navarra, Irúnlarrea 1, E-31008 Pamplona, Spain

^{||}WuXi AppTec (Tianjin) Co. Ltd., TEDA, No. 111 HuangHai Road, fourth Avenue, Tianjin 300456, PR China

S Supporting Information



ABSTRACT: A novel systems therapeutics approach, involving simultaneous inhibition of phosphodiesterase 5 (PDE5) and histone deacetylase (HDAC), has been validated as a potentially novel therapeutic strategy for the treatment of Alzheimer's disease (AD). First-in-class dual inhibitors bearing a sildenafil core have been very recently reported, and the lead molecule 7 has proven this strategy in AD animal models. Because scaffolds may play a critical role in primary activities and ADME-Tox profiling as well as on intellectual property, we have explored alternative scaffolds (vardenafil- and tadalafil-based cores) and evaluated their impact on critical parameters such as primary activities, permeability, toxicity, and in vivo (pharmacokinetics and functional response in hippocampus) to identify a potential alternative lead molecule bearing a different chemotype for in vivo testing.

KEYWORDS: Alzheimer's disease, PDE5, HDACs, dual inhibitor, vardenafil, tadalafil

INTRODUCTION

Phosphodiesterases (PDEs),^{1–4} which are crucial for the degradation of the second messengers cAMP and cGMP, and histone deacetylases (HDACs)^{5,6} have gained much attention as drug targets for neurodegenerative diseases. In Alzheimer's disease (AD), these targets represent an alternative to classical amyloid candidate targets. Among the 11 different phosphodiesterase isoenzymes, inhibition of PDE5 (cGMP-specific) by FDA approved drugs for treating erectile dysfunction like sildenafil (1), vardenafil (2), and tadalafil (3) has been shown to restore cognitive function or/and enhance synaptic plasticity.^{7–9} The underlying mechanism is the activation of gene transcription triggered by protein kinase A (PKA)-dependent phosphorylation of cAMP/cGMP response element-binding (CREB), which is the main modulator for long-term memory (LTM) formation.^{1,5,10,11} HDACs are epigenetic

modulators involved in the deacetylation of lysine residues in histone and other nuclear, cytoplasmic and mitochondrial nonhistone proteins. Acetylation of histones promotes a more relaxed chromatin structure, which triggers transcriptional activation. Several studies have shown that HDACs are implicated in memory processes in mice.^{12–14} More specifically, for class I (HDAC1–3, 8) and class IIb (HDAC6), the specific roles of HDAC isoforms have not been completely elucidated, and it is not fully understood which HDAC isoforms are responsible for the therapeutic effects of pan-HDAC inhibitors observed in AD models.^{12,15}

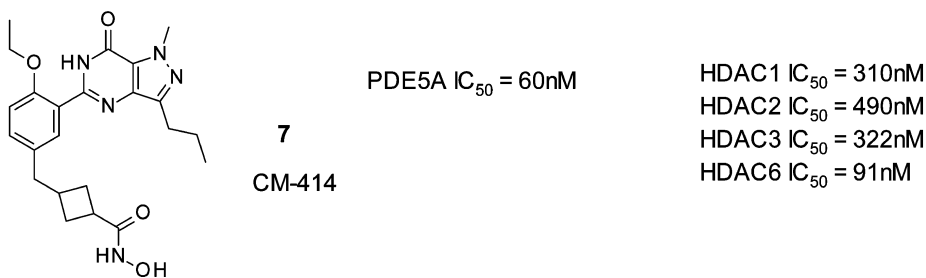
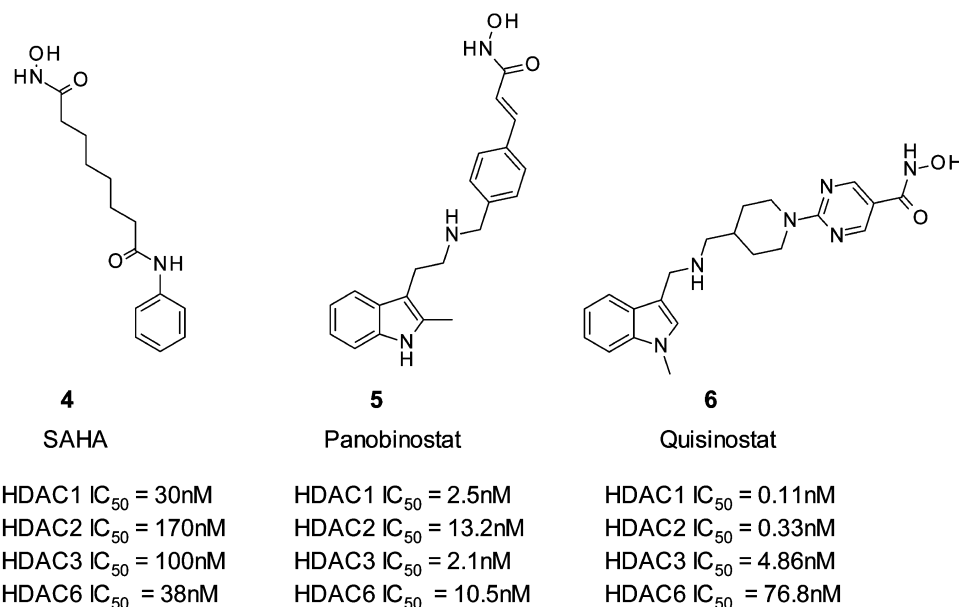
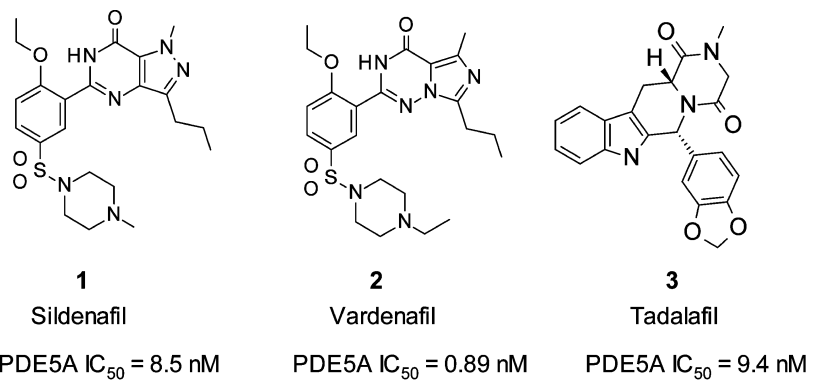
Received: October 31, 2016

Accepted: December 12, 2016

Published: December 12, 2016



Chart 1. Known PDES Inhibitors Shown to Improve Memory (1–3), HDAC inhibitors (4–6), and structure of the Novel Therapeutic Tool 7^a



^aPDES IC₅₀ inhibition values are taken from ref 21 for 1–3. HDAC inhibition IC₅₀ values for 4 are taken from ref 15, while values for 5 were extracted from ref 22 and for 6 from ref 23.

In the last years, therapeutic strategies that target multiple pathological processes in AD have arisen. One approach to achieve this goal is combination therapy. In this sense, we tested the efficacy of combining PDE and HDAC inhibitors in AD mice¹⁶ to demonstrate the validity of a novel therapeutic strategy to treat AD. An alternative to combinatorial therapy is to identify a single chemical compound that targets both protein families. This offers some advantages such as reducing

drug–drug interactions and concurrent pharmacokinetics. With that purpose in mind, we designed a series of novel dual PDES and HDAC inhibitors that led to the discovery of compound 7 (CM-414, Chart 1), which was proven to cross the blood-brain barrier (BBB), induce AcH3K9 acetylation and CREB phosphorylation in the hippocampus, and rescue long-term potentiation (LTP) in APP/PS1 mice.¹⁷ Compound 7 is the result of the derivatization of sildenafil chemotype with a

hydroxamic acid moiety that confers HDAC inhibitory activity following structure-based drug design. In our previous report,¹⁸ we detailed the structure–activity relationship (SAR) exploration of a series of compounds sharing the sildenafil core with different hydroxamic acid moieties that simultaneously inhibit the activity of PDE5 and HDACs. We now present a detailed account of the transference of these HDAC-inhibitory activity conferring R-groups to the chemical structures of vardenafil and tadalafil chemotypes for broader exploration of potency, selectivity and ADME-Tox properties. Aside from enabling enhanced intellectual property (IP) positions, we are also interested in examining how the replacement of the pyrazolo-[4,3-*d*]pyrimidin-7-one core by the vardenafil imidazo[5,1-*f*][1,2,4]triazin-4(3H)-one core affects primary activities as well as ADME properties. According to the sildenafil–vardenafil pair comparison, this scaffold replacement was initially expected to improve PDE5 activity. Regarding HDACs, the impact of the core moiety, which acts as a capping group, might play an anticipator role in primary activity. Moreover, as we have previously observed in other medicinal chemistry projects,^{19,20} enhanced ADME-Tox and selectivity profiles can be attributable to certain chemotypes over others.

RESULTS

According to our proposed mechanism, increased CREB phosphorylation after PDE5 inhibition translates into CREB binding protein (CBP) recruitment, which thereby enhances histone acetylation as CBP has histone acetyl transferase activities. In fact, combinations of **4** (SAHA; Vorinostat, Chart 1) and **3**¹⁶ as well as **4** and **1**¹⁸ exhibited a synergistic increment in acetylated H3K9 in the SH-SY5Y neuroblastoma cell line. Here, this synergistic response was also demonstrated when combining **4** and **2** using AlphaLisa technology. After treating cells with 50 nM **4**, AcH3K9 marks were significantly increased (*P* value < 0.05) when combined with concentrations of **2** higher than 64 nM (1.5-fold change over the vehicle-treated cells) (Figure 1). However, this induction was weaker than that

from well-reported HDAC inhibitors and attached to the piperidinylsulfonamide group of **2**: (1) flexible alkyl linkers from **4** (**13a**), (2) the pyrimidylhydroxamic acid from **6**²³ (Quisinostat, Chart 1) (**13b**), and (3) the cinnamic hydroxamic acid moiety from **5**²² (Panobinostat, Chart 1) (**13c**), to obtain dual inhibitors (Table 1). This transference was rationalized on the basis of the well-established HDACi pharmacophore, which comprises a surface recognition motif at the entrance of the catalytic pocket of HDACs (e.g., the vardenafil core), a linker that accommodates tubular access to the active site and a zinc-chelating moiety (zinc-binding group, ZBG) at the active site (the hydroxamic acid group in this case) (Figure 2A, for the crystal structure of HDAC2 in complex with **4**, PDB entry 4LXZ²⁴). For PDE5, analysis of the binding mode of **2** (PDB entry 3B2R²⁵) revealed that ethylpiperazine orients to the PDE5 surface, meaning that the transferred linker-ZBG would project into the solvent-exposed cavity (Figure 2B) and should not negatively impact PDE5 activity.

These three vardenafil derivatives **13a**–**13c** were synthesized from commercially available 2-(2-ethoxyphenyl)-5-methyl-7-propyl-3*H*-imidazo[5,1-*f*][1,2,4]triazin-4(3*H*)-one (**8**) as shown in Scheme 1. Sulfonyl chloride (**9**) was first prepared by selective sulfonylation at the 5'-position of the phenyl ring; the ethyl esters **10a**–**10c** were obtained by reaction with appropriated amines. Hydrolysis of these esters with LiOH led us to carboxylic acids **11a**–**11c**, which were finally converted into the desired hydroxamic acids by reaction with *O*-(tetrahydro-2*H*-pyran-2-yl)hydroxylamine (THPONH₂) using EDC/HOBt as the coupling system and deprotection under acidic conditions to remove the THP-protecting group.

All three compounds retained potent PDE5 activities (<10 nM), fulfilling our expectations; however, with the exception of compound **13b**, their PDE5 potencies were reduced compared to that of **2**. Thus, the reported higher affinity of **2** (0.89 nM) than **1** (8.5 nM) for PDE5 (Chart 1) was not maintained and a pairwise trend in PDE5 activity between sildenafil-derived¹⁸ and vardenafil-derived compounds was not observed for these three compounds (as illustrated below, Figure 4). This can be attributed to different conformations of the PDE5 H-loop in the different complexes with compounds, as observed for the **1** and **2** cases.²⁵ Regarding HDAC inhibitory activity, these three compounds had different profiles, with compound **13b** being a potent pan-HDAC inhibitor (<20 nM against HDAC1, HDAC2, and HDAC6, although with a certain preference for HDAC1 over the rest of isoforms), compound **13a** in the middle-nanomolar range against HDAC1 and HDAC6 and compound **13c** having micromolar activities against HDAC1 and HDAC6. Of note, HDAC1 (with neuroprotective activity²⁶), HDAC2 (a transcriptional repressor of CREB-regulated genes^{27,28}), and HDAC6 (involved in α -tubulin acetylation and thereby with potential in the amelioration of tau^{29,30} and amyloid pathologies^{31,32}) isoforms were routinely included in our screening panel. Finally, as HDAC3³³ is a critical negative regulator of long-term memory formation, its inhibitory activity was also assayed for selected compounds.

The good HDAC potency conferred by the pyrimidylhydroxamic moiety (**13b**) is consistent with our previous results for sildenafil-derived compounds,¹⁸ **6** and related analogues.^{23,34} In order to prevent cytotoxicity associated with potent class I HDAC inhibition (see below the case of **13b**), we concentrated on modifications leading to midnanomolar inhibitors ($IC_{50} > 100$ nM, such as **13d**) instead of further exploring analogues of low nanomolar inhibition such as **13b**.

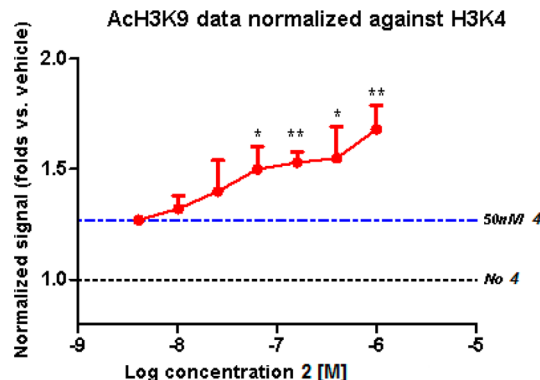
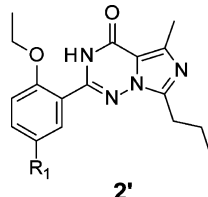


Figure 1. Detection of AcH3K9 assayed using SH-SY5Y cells and AlphaLisa technology. SH-SY5Y cells were treated with **4** and **2** for 2 h (**p* ≤ 0.05 and ***p* ≤ 0.01).

obtained for the combination of **4** and **1**.¹⁸ For example, at a concentration of 1 μ M of each PDE5 inhibitor with 50 nM of **4**, **1** achieved a 2.1-fold¹⁸ increase in AcH3K9 marks compared to the 1.7-fold increase obtained by **2** (Figure 1).

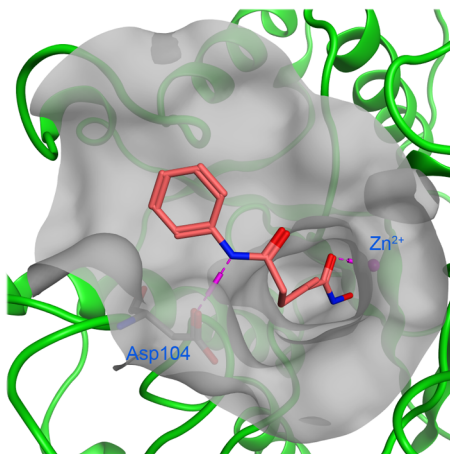
After validating the mechanism with the **2**–**4** combination and following a similar strategy for **1**,¹⁸ the following different linker moieties bearing a hydroxamic acid group were extracted

Table 1. Initial Set of Dual PDE5-HDAC-Targeting Inhibitors Based on Vardenafil



Cpd	R1	PDE5A IC ₅₀ nM	HDAC1 IC ₅₀ nM	HDAC2 IC ₅₀ nM	HDAC6 IC ₅₀ nM
13a		1	153	2080	345
13b		0.2	1	13	19
13c		6	4640	>20000	1050
13d		3	175	2690	111

A) HDAC2 - 4 complex



B) PDE5 - 2 complex

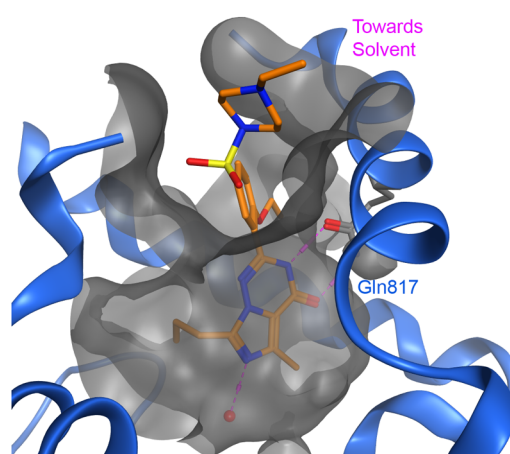
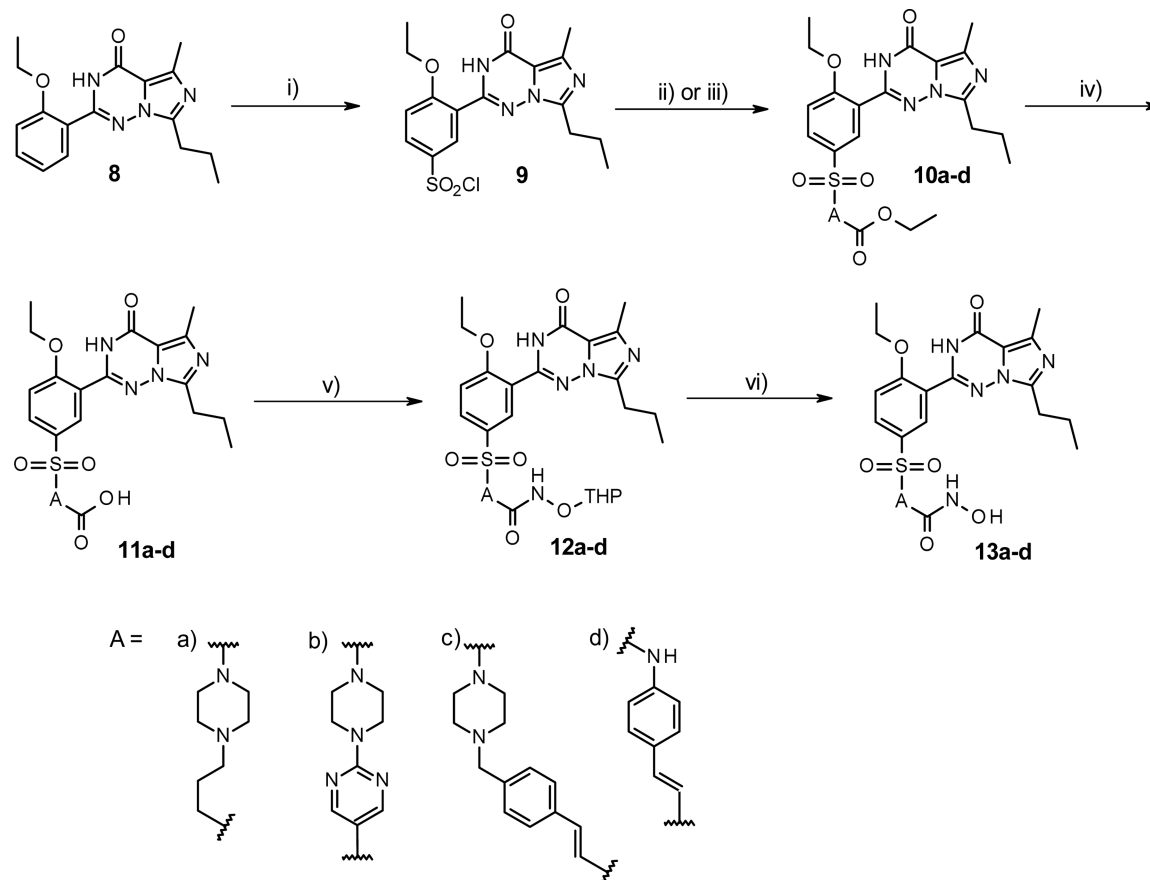


Figure 2. (A) **4** and HDAC2 complex (PDB entry 4LXZ²⁴). The NH from the **4** amide group makes a H-bond contact with the well-conserved residue Asp104 from HDAC2 (Asp99 for HDAC1 and Asp567 for HDAC6). (B) Crystal structure of **2** in the PDES cavity (PDB entry 3B2R²⁵). The vardenafil imidazotriazine core forms a bidentate H-bond with the conserved Gln817, and the ethylpiperazine is solvent-oriented.

The HDAC inhibitory activity of the cinnamic acid moiety was recovered by replacing the piperidine group of **13c** with a flexible smaller secondary amine (**13d**). In fact, as predicted by our docking studies (Figure 3) and confirmed by experimental data (Table 1, above), **13d** was able to achieve key interactions at HDAC binding site (as illustrated with HDAC2, Figure 3A,B) as well as at PDES binding site (Figure 3C,D) leading to

an adequate dual inhibition: PDES in low nanomolar ($IC_{50} < 10$ nM) and HDACs in midnanomolar ($IC_{50} > 100$ nM). This compound was prepared according to the same synthetic strategy described for **13a–13c** (Scheme 1). According to our docking studies, the piperazine ring of **13c** projects into a rim surface hydrophobic area, and the vardenafil core protrudes out of the protein, establishing fewer contacts with the protein than

Scheme 1^a

^aConditions: (i) ClSO_3H , 0 °C, then rt for 2 h; (ii) corresponding amine, Et_3N , EtOH, 100 °C MW for 1 h; (iii) ethyl (*E*)-3-(4-aminophenyl)prop-2-enoate, pyridine, rt, overnight; (iv) $\text{LiOH}\cdot\text{H}_2\text{O}$, THF/MeOH/ H_2O (10:1:5), rt, overnight; (v) EDC·HCl, HOBt, THPONH₂, NMM, DMF, rt, overnight; and (vi) HCl, 1,4-dioxane (2.0 or 4.0 M), rt for 3 h.

can explain the reduced potency of **13c** compared to **13d**, whose vardenafil capping group is predicted to orient toward the L1 loop, overlapping well with **4** (Figure S1A,B). For both compounds, the cinnamic acid moiety phenyl ring lies flanked by the well-conserved aromatic residues Phe150 (HDAC1; Phe155 in HDAC2; and Phe620 in HDAC6) and Phe205 (HDAC1; Phe210 in HDAC2; and Phe680 in HDAC6) at the entrance of the catalytic channel. This encouraged us to reduce the linker size and decrease its polar surface area (PSA) by designing carbon-linked substituents at the 5'-position of the phenyl ring (**19**, **22**, **23**, **27**, **27a**, and **27b**, Table 2) with different flexibilities and the goal of improving the permeability and thereby CNS penetration. This examination was very focused and restricted to those substituents previously introduced in the sildenafil-derived series and for which potent compounds were identified.¹⁸

Compounds **19**, **22**, and **23** were synthesized as illustrated in Scheme 2. Iodide **14**, which was obtained after reaction of **8** with NIS, was first transformed into boronic ester **15**, which reacted with methyl (*E*)-3-[4-(bromomethyl)phenyl]prop-2-enoate through a palladium coupling reaction to afford methyl ester **16**. Then, carboxylic acid **17** was obtained by reaction with LiOH, and the desired hydroxamic acid **19** was prepared with the THP-protected intermediate **18**. Cyclobutyl derivatives **22** and **23** were also prepared from iodide **14**. In this case, ethyl ester **20** was synthesized by a palladium catalyzed cross coupling reaction with ethyl 3-(9-borabicyclo[3.3.1]nonan-9-

ylmethyl)cyclobutanecarboxylate and the corresponding carboxylic acid **21** was then afforded through hydrolysis. Compound **22** was directly prepared by reaction of **21** with hydroxylamine and compound **23** using *N,N*-dimethylhydroxylamine.

Compound **27** was prepared through a similar route (Scheme 3). Starting from boronic ester **15**, ethyl ester **24** was synthesized by reaction with the corresponding trifluoromethanesulfonyl derivative and catalytic hydrogenation. Then, the desired hydroxamic acid **27** was obtained by the following previously described three-step protocol: (1) hydrolysis, (2) reaction with THPONH₂, and (3) acidic deprotection. In this case, pure isomers **27a** and **27b** (*cis*- and *trans*-) were also isolated after preparative HPLC purification of the crude reaction mixture, though their stereochemistry could not be confirmed, and they are randomly assigned.

Compounds in Table 2 were, with the exception of compound **22**, low micromolar inhibitors of HDAC1 and HDAC2 (or inactive like **27**, **27a**, and **27b**), with a higher variety of potencies against HDAC6 (middle-nanomolar to micromolar). Of note, a significant difference in HDAC6 activity was observed between the two enantiomers (**27a** and **27b**, IC_{50} of 673 and 9840 nM, respectively) of the racemic compound **27** (2110 nM). HDAC6 was the only primary activity influenced by the stereochemistry of this compound. Compound **22**, the corresponding vardenafil-matched-pair of our lead compound **7**, had a very promising primary profile and

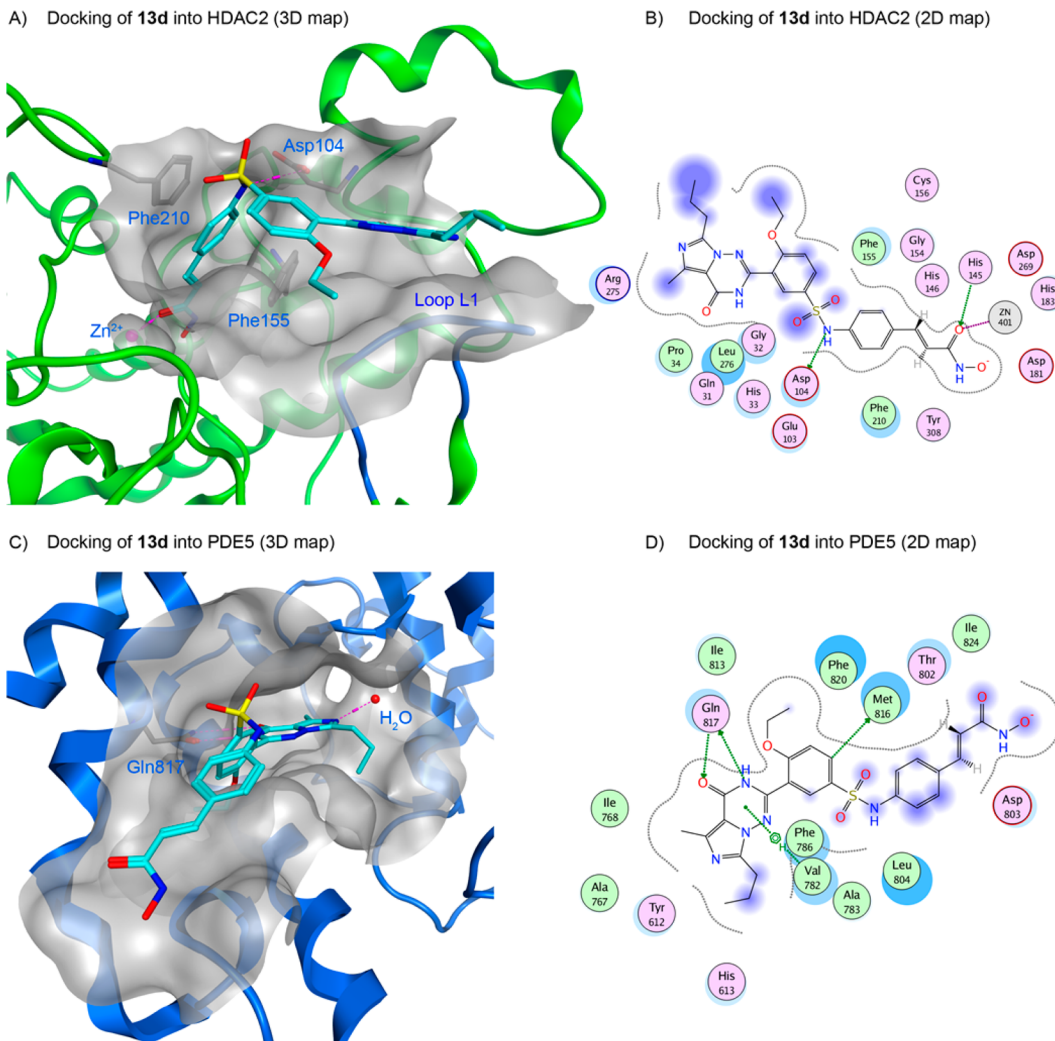


Figure 3. (A) Docking of **13d** (blue sticks) into the catalytic pocket of HDAC2. (B) 2D map interactions of **13d** with HDAC2. (C) Docking of **13d** into the catalytic pocket of PDE5. (D) 2D map interactions of **13d** with PDE5. In panels (C) and (D), green lines correspond to hydrogen bonds with the side chain of the corresponding amino acid acting as an acceptor and violet areas to solvent exposed areas of the docked compound.

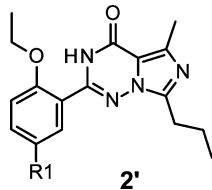
satisfied our initial requirements for a lead compound; it displayed a moderate class I HDAC inhibitory profile (IC_{50} against HDAC1 and HDAC2 of 286 and 1260 nM, respectively) and potent HDAC6 affinity (IC_{50} of 110 nM). In fact, compound **22** is predicted by docking to establish an optimal chelation arrangement with its hydroxamic acid group to coordinate with Zn metal, as **13d** does (Figure 3A), superposing extremely well with that observed for **4** in its corresponding crystal structure complexed with HDAC2 (Figure S1C). Compound **23** was synthesized to confirm the impact of the hydroxamic acid moiety by replacing it with the corresponding hydroxamate ester, and as expected, it was inactive against all three HDAC isoforms.

The heat map in Figure 4 explicitly shows the impact of scaffold replacement on primary activities (IC_{50}) and toxicity (LC_{50}) by direct comparison between matched-pairs: vardenafil-derived compounds (**13a–13d**, **19**, and **22**) vs previously reported molecules bearing the sildenafil core.¹⁸ Their pIC_{50} differences (ΔpIC_{50}), against each target (PDE5 and HDACs), as well as their differences in cytotoxicity (ΔpLC_{50}) are represented in the heat map (Figure 4). For PDE5, compounds **19** and **22** recovered the higher affinity of **2** over **1** (the more positive the pIC_{50} difference in Figure 4, the higher affinity for

vardenafil- over sildenafil-derived molecules and vice versa), though as stated above, this was not a general trend for all of the compounds (e.g., **13a**, **13c**, and **13d**). Regarding HDACs, no significant differences between both series could be acknowledged, with the exception of compounds **13b** and **13c**. Here, the vardenafil-derived compound **13b** was ~1 log unit more active against all three HDAC isoforms than its corresponding sildenafil-pair (corresponding pIC_{50} values are reported in the Supporting Information, Figure S2). However, the opposite trend was shown by the vardenafil-derived compound **13c** against HDAC6. Considering all of the data in Figure 4, there is no evidence to support a preference for a given HDAC capping group (**1** or **2**); additionally, the vardenafil core does not always lead to higher affinities for PDE5. Altogether, these data suggest the presence of nonadditive effects for these chemical series against the primary activities.³⁵

On the other hand, taking into account that other phosphodiesterase isoforms such as PDE9 and PDE6 also hydrolyze cGMP, the effects of **7** and **22** on these two targets were tested. In fact, **7** does not inhibit PDE9 ($IC_{50} > 10 \mu M$);¹⁷ but, its activity vs PDE6 is quite potent (IC_{50} is 2.6 nM).¹⁸ Compound **22** is even better inhibitor of PDE6 than **7** (around

Table 2. Focused Exploration of the Dual PDE5-HDAC Targeting Inhibitors Based on 2



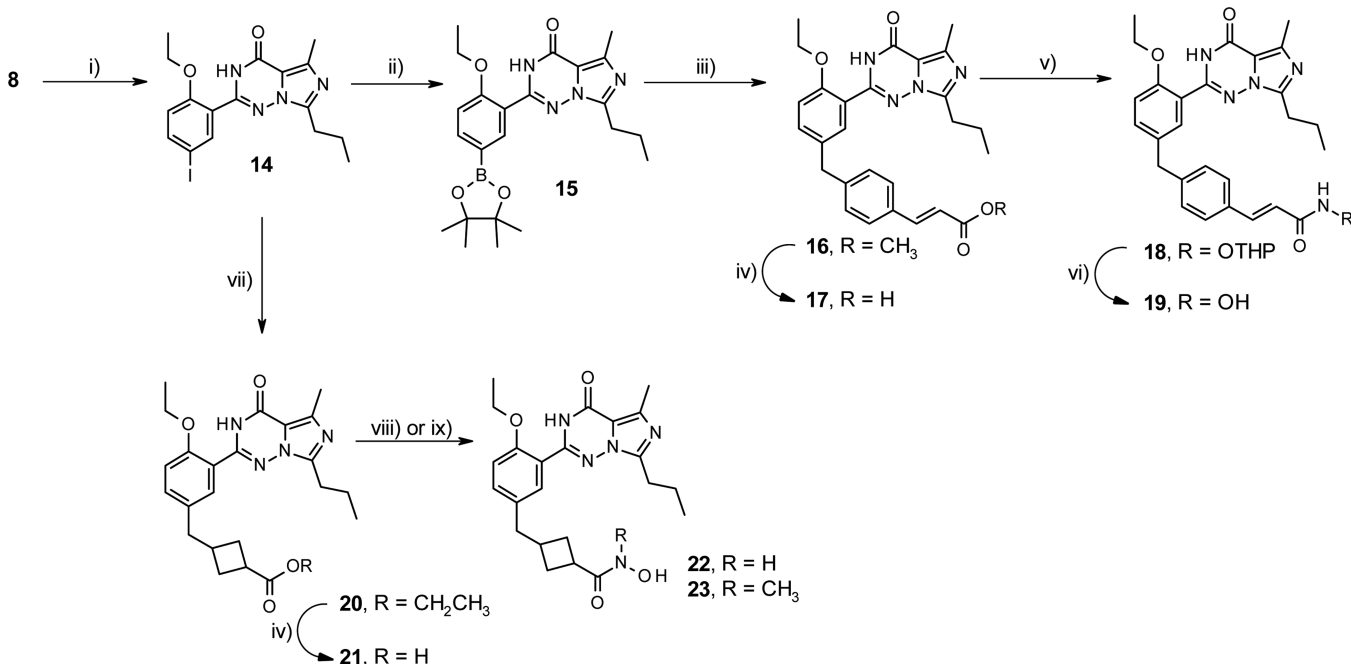
Cpd	R1	PDE5A IC ₅₀ nM	HDAC1 IC ₅₀ nM	HDAC2 IC ₅₀ nM	HDAC3 IC ₅₀ nM	HDAC6 IC ₅₀ nM
19		8	1250	8310		487
22		5	286	1260	854	110
23		6	>20000	>20000		>20000
27		7	3790	>20000		2110
27a		6	2470	>20000		673
27b		10	7860	>20000		9840

1 log unit), its IC₅₀ is 0.27 nM; however, as 7, 22 does not either inhibit PDE9 (its IC₅₀ > 10 μM). Additionally, considering that PDE3A is a phosphodiesterase isoform that hydrolyses cAMP and cGMP and is involved in cardiac contractility³⁶ (its inhibition may lead to unwanted cardiac side-effects), we also tested these two molecules 7 and 22 vs PDE3A to assess the potential impact of central core replacement from cardiovascular safety perspective. Compound 7 shows a moderate inhibition against PDE3A (IC₅₀ is 1.8 μM)¹⁸ whereas 22 inhibits PDE3A at midnanomolar range (IC₅₀ is 620 nM).

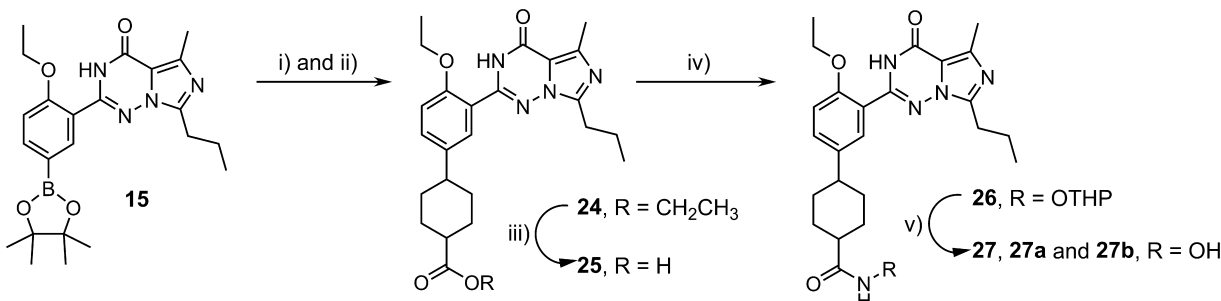
A similar strategy as followed for 1¹⁸ and 2 (Tables 1 and 2, respectively) was applied to the molecule of 3 (Table 3). Analysis of the crystal structure of 3 into PDES (Figure 5, PDB entry 1XOZ³⁷) led us to design dual PDES and HDAC inhibitory compounds by appending the linker-ZBG moiety at the N2-Me of the piperazinedione ring, which orients toward the solvent-exposed surface. Here, to avoid formation of labile nitrogen–nitrogen bonds (even if chemically feasible), the

piperidine ring of the transferred R-groups was replaced by piperazine (compounds 40a–40c).

Compounds were initially prepared as mixtures of diastereoisomers following the synthetic route outlined in Scheme 4. Commercially available 1,3-benzodioxol-5-ylmethanol (28) was first oxidized to piperonal with MnO₂, and then compound 31 was synthesized following a known synthetic procedure.³⁸ The stereochemistry of this intermediate has been previously studied and was confirmed to be the 6*R*/12*aR* *cis* isomer. Nevertheless, the subsequent transformations have not been described before, and as it is known that both stereogenic centers in the tadalafil core can epimerize³⁸ and their stereochemistries have not been studied, the compounds are described as a mixture of diastereomers. From intermediate 31, BOC-protected piperidines 35a and 35b were obtained followed by ethyl esters 37a–37d after removal of the BOC-protecting groups and substitution with the corresponding chloride, bromide or mesylate derivatives. Finally hydroxamic acid 40a was directly prepared using hydroxylamine and

Scheme 2^a

^aConditions: (i) NIS, TFA, 0 °C, then rt, overnight; (ii) 4,4,5,5-tetramethyl-2-(4,4,5,5-tetramethyl-1,3,2-dioxaborolan-2-yl)-1,3,2-dioxaborolane, Pd(dppf)Cl₂, KOAc, 1,4-dioxane, 90 °C, overnight; (iii) methyl (E)-3-[4-(bromomethyl)phenyl]prop-2-enoate, Pd(PPh₃)₄, K₂CO₃, 1,4-dioxane/H₂O (5:2), 85 °C, MW for 1 h; (iv) LiOH-H₂O, THF/MeOH/H₂O (3:3:2), rt, overnight; (v) EDC·HCl, HOEt, THPONH₂, NMM, DMF, rt, overnight; (vi) HCl/EtOAc (2.0 M), rt for 1 h; (vii) ethyl 3-(9-borabicyclo[3.3.1]nonan-9-ylmethyl)cyclobutanecarboxylate, Pd₂(dba)₃, xantphos, Na₂CO₃, 1,4-dioxane/H₂O (5:1), reflux, overnight; (viii) NH₂OH·HCl, DIEA, BOP, DMF, rt, overnight; and (ix) EDC·HCl, HOEt, N,O-dimethylhydroxylamine, NMM, DMF, rt, overnight.

Scheme 3^a

^aConditions: (i) ethyl 4-(trifluoromethylsulfonyloxy)cyclohex-3-ene-1-carboxylate, K₂CO₃, Pd(PPh₃)₄, 1,4-dioxane/H₂O (6:1), 80 °C, overnight; (ii) Pd/C, H₂ (1 atm), EtOAc, rt for 3 h; (iii) LiOH-H₂O, MeOH/THF/H₂O (1:3:1), rt, overnight; (iv) EDC·HCl, HOEt, THPONH₂, NMM, DMF, rt, overnight; and (v) HCl/EtOAc (1.0 M), rt for 1 h.

hydroxamic acids **40b**–**40d**, which were prepared using a previously described strategy (hydrolysis, reaction with THPONH₂ and deprotection under acidic conditions).

In contrast, Nortadalafil **32** (stereochemistry previously studied) was obtained after treatment of intermediate **31** with ammonia. Next, reaction with ethyl (E)-3-(4-iodophenyl)prop-2-enoate under basic conditions led us to ethyl ester **33**, which was finally converted into hydroxamic acid **34** using hydroxylamine.

Once again, our hypothesis for dual-acting compounds was validated for tadalafil derivatives (Table 3), identifying compounds **40b** and **40c** in the middle-nanomolar range activities for HDAC1 and HDAC6 and in the low micromolar range activity against HDAC2. The flexible linker in derivative **40a** was detrimental for HDAC activity. The PDES activity of

all three compounds was compromised, with a drop of approximately 1.2–1.9 log units compared to **3** (IC₅₀ of 9.4 nM), Chart 1. This potency drop can be attributed at least in part to the fact that compounds **40a**–**40c** are a mixture of diastereoisomers, while the stereochemistry of **3** is *cis*-(6*R*,12*aR*); this absolute stereochemistry has been proven to be crucial for the PDES inhibitory activity,³⁹ especially the R absolute configuration at position-6, as the 1,3-benzodioxole group enters the hydrophobic pocket occupied by the sildenafil and vardenafil ethoxy group (Figures 2A and 5). Shortening of the linker of derivative **40c** by removal of the piperazine ring (**34**) abolished its HDAC activity; therefore, small linker-ZBG groups were not further examined for the tadalafil core. Based on the good HDAC potency of the pyrimidylhydroxamic acid **40b**, a homologated derivative **40d** was prepared, with a slight

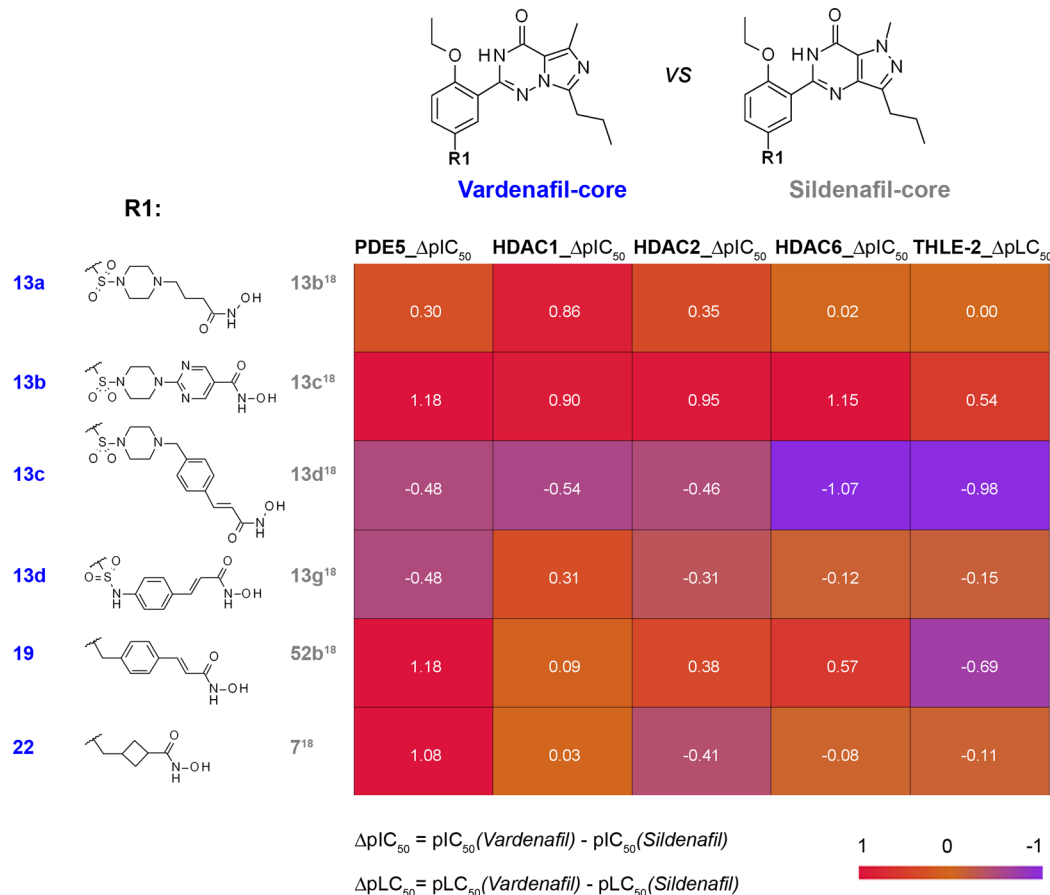


Figure 4. Heat map with pIC_{50} differences between the matched-pair compounds for vardenafil-derived compounds (**13a**–**13d**, **19**, and **22**), reported in this paper, and sildenafile-derived compounds already described in a previous manuscript.¹⁸ Cell values correspond to the pIC_{50} (or pLC_{50} for cytotoxicity against THLE-2) values between the corresponding vardenafil-derived compound and its corresponding matched sildenafile-derived pair, with positive values (tending to 1) indicating higher affinities (or higher cytotoxicities) for the vardenafil-derived compounds and vice versa. pIC_{50} (or pLC_{50}) differences below 0.3 are regarded within the experimental error. Compound numbers next to R1 groups correspond to vardenafil-based derivatives (blue) described in this manuscript and those in gray are for the sildenafile-derivatives.¹⁸

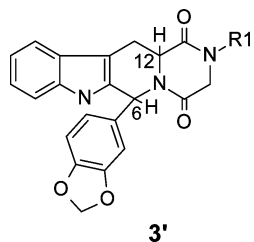
improvement in activity against all four targets. As compound **40d** had the highest potency among all of the compounds in Table 3 (IC_{50} of 68 and 77 nM against HDAC1 and HDAC6, respectively), its corresponding stereochemistry was carefully determined by NMR, demonstrating that it corresponds to the *trans* form, although in the absence of further studies, the absolute stereochemistry of the 6- and 12- centers cannot be resolved and we cannot ensure that a single unique enantiomer is present. Potent PDE5 activity was not recovered because of the existence of a mixture of enantiomers (with both *R*- and *S*-configurations at position-6). This decreased PDE5 potency, and the synthetic effort to isolate absolute enantiomers was regarded as a drawback of the tadalafil-derived compounds compared to the sildenafile- and vardenafil-based derivatives.

Cytotoxicity and Cellular Functional Response: Effects on Histone Acetylation and CREB Phosphorylation. For each series, the most potent compounds against PDE5 and at least one HDAC isoform were moved into cellular assays aimed at evaluating their cytotoxicity and functional response in inducing H3K9 and tubulin acetylation as well as phosphorylation (pCREB) marks. The cell viability of transformed human liver epithelial cells (THLE-2) following a 72 h exposure to test compounds was chosen as an indicator of cytotoxicity. Very potent HDAC class I ($\text{IC}_{50} < 10$ nM) inhibitors showed strong antiproliferative responses against

THLE-2 (**13b**, $\text{LC}_{50} = 419$ nM, Table 4), while those with midnanomolar or weaker class I HDAC activity demonstrated an acceptable security profile, with LC_{50} values close to or higher than 10 μM , as in the case of the remaining vardenafil-based derivatives in Table 4 (**13d**, **19**, **22**, **23**, **27a**). Tadalafil-based compounds exhibited midlevel (1000–5000 nM) cytotoxicities similar to **4** (3590 nM), which, based on its tolerance in *in vivo* efficacy models,¹⁶ was regarded as our goal reference for an acceptable minimal therapeutic window. As seen in Figure 4, in the cases of **13b**, **13c**, and **19** and their corresponding matched-pairs bearing sildenafile scaffold, central core replacement shows a clear impact on THLE-2 cytotoxicity in both directions (suggesting nonadditive effects) and HDAC-1 independent (at least, according to data for **19**); however, further exploration is required to make any assessment about the scaffolds and THLE-2 cytotoxicity.

Western blotting assays with antibodies raised against acetylated H3K9 and tubulin-K40 in SH-SY5Y neuroblastoma cells were also routinely carried out for selected compounds at three different concentrations (100, 500, 1000 nM) after 2 h of incubation (Table 4). Compound **23** was regarded as a negative control to determine the minimum significantly quantifiable response in gels. A certain dose-dependent response against both markers, with values greater than 1 that indicated acetylation induction, was observed for most of the compounds

Table 3. Dual PDES-HDAC-Targeting Inhibitors Based on 3



Cpd	R1	PDE5A	HDAC1	HDAC2	HDAC6
		IC₅₀ nM	IC₅₀ nM	IC₅₀ nM	IC₅₀ nM
40a		135	>20000	>20000	2520
40b		653	197	1360	239
40c		721	721	7350	242
34		115	>20000	>20000	>20000
40d		308	68	623	77

in Table 4, especially those (19, 22, 27a, 40c) having moderate PAMPA permeability (with Pe values between 10 and 30 nm/s), as determined using a brain polar lipid (BPL) membrane suitable for predicting brain permeability. These four most potent compounds in Table 4 greatly induced Tubulin-K40 acetylation at 1 μ M (a dose surpassing its midnanomolar HDAC6 IC₅₀ value), with fold increases over nontreated cells ranging from 4.1 to 18.7. However, only three of these molecules (19, 22 and 27a) achieve a minimal therapeutic window of 1 log unit considering their LC₅₀ in THLE-2 cells. Derivatives 19 and 27a are low micromolar HDAC1 inhibitors (Table 2) and are only able to induce low levels of AcH3K9 (3.6 and 2.6 respectively at 1 μ M) compared to 4 and 7 (13.9 and 19.9, respectively, at the same dose).

The effect on the AcH3K9 mark exerted by compound 22 (1.6 fold at 1 μ M) was weaker than initially expected according to its HDAC1 inhibitory potency and permeability, especially when compared to its sildenafil-matched-pair 7. This differential response between 22 and 7 was also confirmed using

AlphaLisa technology. Using this assay, compound 22 achieved a significant increase in AcH3K9 mark up to 400 nM (*P* value <0.05), with a maximum response of 1.5-fold at 1 μ M (Supporting Information, Figure S3). In contrast, under the same conditions, 7 elicited a significant response from 64 nM, reaching a maximal AcH3K9 fold increment of 3.4 at 1 μ M.¹⁷ With similar HDAC1 inhibitory activities (286 and 310 nM for 22 and 7, respectively) and permeabilities (10.9 vs 15.7 nm/s), the slightly reduced potency of 22 compared to 7 against HDAC2 (IC₅₀ of 1260 nM vs 490 nM) and HDAC3 (IC₅₀ of 854 vs 322 nM) can, in part, explain this differential functional cellular response, especially if taking into account that the particular contribution of each HDAC to H3K9 deacetylation remains unknown and that the full isoform selectivity profile of compound 22 (e.g., against HDAC8) was not determined and compared to 7.

Moreover, solubility differences between both compounds (Table 5), with compound 22 having poor to moderate solubility (7.84 μ g/mL at pH = 7.4), may also play a role.

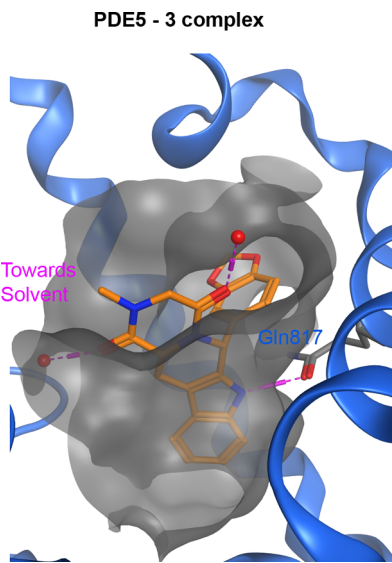


Figure 5. 3 and PDES complex (PDB entry 1XOZ³⁷) with the conserved H-bond with Gln817.

Phosphorylation of CREB-Ser133 in SH-SY5Y neuroblastoma cells after treatment with selected compounds at 500 nM, and different incubation times (30 min and 2 h), was quantified as an indicator of PDES inhibition at the cellular level (Table 4). Compared to the effects promoted by 1 (1.9-fold increase at 30 min) and 3 (1.4-fold after 2 h), 2 showed a weaker, but noticeable response (1.2-fold after 2 h) that also highlights the influence of the incubation time on the detection of increased pCREB. Most compounds in Table 4 had a minor response at the chosen incubation times, with only a few remarkable exceptions (e.g., compound 27a).

Functional Response of Compound 22 in Tg2576 Neurons and ADME Properties. Based on its acceptable cellular profile and for comparison purposes between the sildenafil- and vardenafil-derived series, compound 22 was further moved into assays using primary cultures of Tg2576 neurons. To achieve a notable induction in AcH3K9 (300%) and pCREB (100%) over nontreated Tg2576 neurons, it was necessary to increase the dose of compound 22 from 100 nM (no functional response at this concentration) to 500 nM (Table 5). This 100 nM dose of 22 was able to increase the measured levels of AcTub by 50% over nontreated Tg2576 neurons, yielding a similar response to 7 (40%). Finally, we analyzed the effect of compound 22 on the AD-related markers human amyloid precursor protein (hAPP) processing and tau phosphorylation (pTau) in Tg2576 neurons. hAPP processing by the amyloidogenic pathway was determined through Western blotting by evaluating the expression of the 99-amino-acid-long APP-carboxy-terminal fragments (APP-CTFs), designated C99, which is the A β 42 precursor. Following 72 h of incubation, compound 22 induced a decrease of 25% and 48% in C99 levels at 100 nM and 500 nM, respectively. pTau levels were determined by a phospho-specific AT8 antibody that recognizes hyperphosphorylated Ser202/Thr205 epitopes. A greater dose of compound 22 was required to achieve an observable reduction in pTau levels (11% at 500 nM). In summary, the vardenafil-derived compound 22 elicited an in vitro functional response on Tg2576 neurons in full agreement with its expected mechanism of action; however, it was less efficient than its sildenafil-matched-pair 7¹⁷ (Table 5). To

establish its therapeutic window, the cytotoxicity of compound 22 in primary neuronal cultures of glia cells and peripheral blood mononuclear cells (PBMCs obtained from healthy donors) was also determined, yielding a LC₅₀ value of 6.1 and 6.2 μ M (Table 5), respectively. This translates into a minimal therapeutic window, greater than 1 log unit, considering a dose of 500 nM for achieving cellular functional response. Thus, from the viewpoint of in vitro functional efficacy in primary neuronal culture (Tg2576 neurons) and toxicity, compound 7 outperforms compound 22.

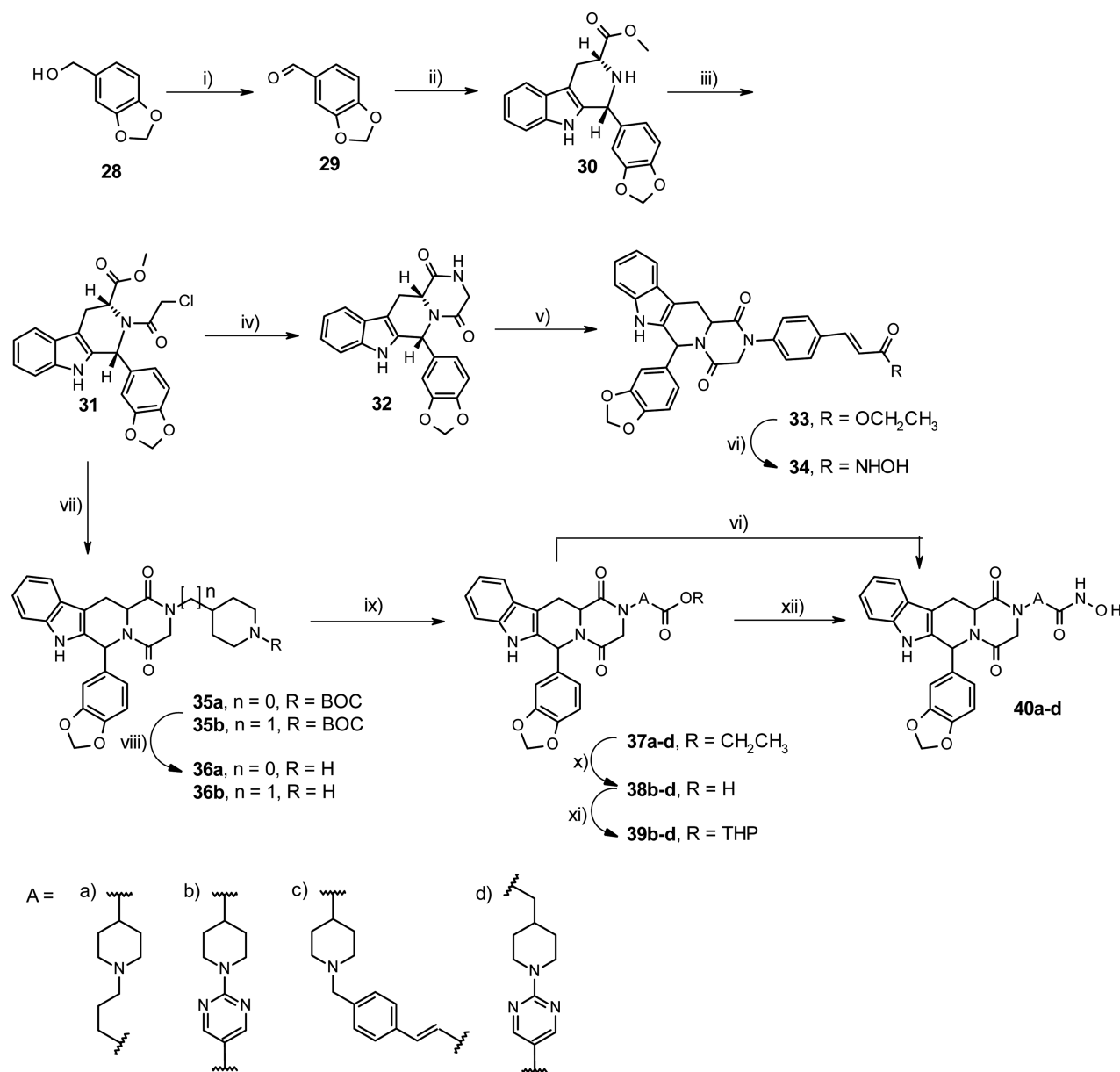
Table 5 also presents preliminary in vitro ADME data for compound 22 compared to ref 7. Compound 22, as well as the sildenafil analogue 7, showed low inhibition of the major cytochrome P450 isoforms (1A2, 2C19, 2C9, 2D6), with percent inhibition values at 10 μ M less or close to 50% and with potent inhibition (97.1%) of the 3A4 isoform at this concentration (the isoform mainly involved in the metabolism of PDES inhibitors).⁴⁰ We also determined the in vivo CNS penetration in mice of compound 22 after intraperitoneal administration at a dose of 40 mg/kg by determining the logBB, where BB is the ratio of the brain to plasma concentration. Similar to compound 7, compound 22 revealed poor central access with a 15 min logBB value of -1.9 , which is probably attributable to its high polar surface area; in agreement with their moderate passive diffusion determined by PAMPA assay. Taking all of these ADME results into account, we can conclude that vardenafil-derived 22 shares a worse ADME profile than its sildenafil-derived analogue, 7; in fact, according to a well-established solubility ranking,⁴¹ molecule bearing the vardenafil core 22 shows a sparingly solubility (<10 μ g/mL) but 7 is partially soluble (its solubility value is between 10 and 100 μ g/mL).

Then, to explore whether compound 22 achieves a functional response in the CNS, a 40 mg/kg dose was administered intraperitoneally, and pCREB-Ser133 phosphorylation marks in the hippocampus were quantified after 15, 30, and 60 min. A small pCREB increment (25% over nontreated) was detected at 1 h postadministration, meaning a weak induction in comparison to that obtained for compound 7 (Table 5).

CONCLUSIONS

Scaffold replacement is an important strategy in medicinal chemistry, not only from an intellectual property (IP) perspective but also to achieve a better biochemical profiling (in terms of primary activity and/or off-target selectivity) as well as to improve ADME-Tox properties versus other chemical series.^{19,20} Then, considering our previous findings with compounds bearing the sildenafil core, targeting PDES and HDACs proteins,¹⁸ we explored known alternative scaffolds (tadalafil and vardenafil chemotypes) to discover potent dual acting compounds able to improve our current lead molecule 7¹⁸ for in vivo testing.

Our scaffolds exploration showed that compounds from both chemical series, vardenafil- and tadalafil-derived molecules, exhibited cellular functional activity at inducing H3K9 and tubulin acetylation and promoting CREB phosphorylation in SH-SY5Y neuroblastoma cells, but to a lesser extent than our previously described lead compound CM-414 7.^{17,18} Its corresponding vardenafil-based matched-pair derivative, compound 22, shares a similar ADME profile with 7 (more importantly, similar CNS penetration), though reduced solubility. On the other hand, compared to 7, compound 22 exhibits less induction of functional hallmarks and a diminished

Scheme 4^a

^aConditions: (i) MnO_2 , CH_2Cl_2 , rt, overnight; (ii) (R)-methyl 2-amino-3-(1*H*-indol-3-yl)propanoate, propan-2-ol, reflux, overnight; (iii) chloroacetyl chloride, Et_3N , THF, 0 °C, then rt for 3 h; (iv) NH_3/MeOH (30%), 40 °C, 3 days; (v) (\pm)-trans-1,2-diaminocyclohexane, ethyl (E)-3-(4-iodophenyl)prop-2-enoate, K_3PO_4 , CuI , 1,4-dioxane, rt, 8 days; (vi) $\text{NH}_2\text{OH}/\text{MeOH}$ (2.0 M), NaCN , 50 °C for 3 h; (vii) corresponding amine, MeOH , 80–90 °C, 3 days; (viii) TFA, CH_2Cl_2 , rt, 2 h; (ix) corresponding bromide, chloride or mesylate, K_2CO_3 , KI (optional), CH_3CN , rt for 5–12 h; (x) $\text{LiOH}\cdot\text{H}_2\text{O}$, $\text{THF}/\text{H}_2\text{O}$ (2:1, 3:1 or 3:2), rt, overnight; (xi) EDC·HCl, HOEt, THPONH₂, NMM, DMF, 30 °C, overnight; and (xii) $\text{HCl}/1,4\text{-dioxane}$ (1.0 or 3.0 M), rt, overnight.

capacity to reduce AD-related markers in vitro in primary neuronal culture (Tg2576 neurons). This correlates well with in vivo measured incremented levels of pCREB after administering the same dose for both compounds which show a similar PK profile and brain penetration (Table 5).

Therefore, all together, the narrower therapeutic range of compound 22, based on its weaker functional efficacy and its higher in vitro cytotoxicity in glia neurons and PBMCs, as well as worse off-target selectivity profiling and poorer in vivo pCREB efficacy than sildenafil-analogue 7 prompted us to not progress 22 further to in vivo models of AD. In vitro, therapeutic window, and in vivo, functional mark at CNS, data suggest sildenafil-core as the most adequate scaffold for these

dual acting molecules to treat AD. However, there is still a broad alternative of chemotypes to sildenafil-core ready to be explored,⁴² as we did with vardenafil- and tadalafil-scaffolds.

From a medicinal chemistry perspective, this scaffold replacement study case emphasizes the role of the chemotype in achieving differential primary activities and cytotoxicity profiles (Figure 4) as well as ADME properties (e.g., solubility, Table 5) beyond intellectual property. Thus, reported results highlight the impact of the chemotype to identify the most appropriate chemical probe to validate a novel therapeutic approach in vivo, derisking the proposed systems therapeutics strategy and, consequently, to progress/discard a new drug discovery project.

Table 4. Functional Cellular Profile of Selected Inhibitors^a

compd	THLE-2, LC ₅₀ (nM)	AcH3K9 levels (fold-change over basal (1)) (100, 500, 1000 nM)	AcTub levels (fold-change over basal (1)) (100, 500, 1000 nM)	pCREB levels (fold-change over basal (1)) at 500 nM, 30 min, 2 h	PAMPA, <i>P</i> _e (nm/s)
1	>100 000	N.D.	N.D.	1.9 0.6	27.5
2	>100 000	N.D.	N.D.	0.9 1.2	21.4
3	60 300	N.D.	N.D.	1.3 1.4	26.8
4	3590	4.0 12.5 13.9	5.0 11.9 27.6	N.D.	2.34
7 ¹⁸	7200	1.2 7.4 19.9	1.5 12.7 17.8	1.5 1.2	15.7
13b	419	0.8 0.7 1.4	0.9 1.4 0.9	1.1 2.3	N.D.
13d	39 100	0.8 0.4 0.4	1.2 1.1 1.9	N.D.	2.1
19	11 700	0.8 3.7 3.6	0.2 2.6 4.1	N.D.	15.7
22	9370	0.8 1.4 1.6	1.4 3.4 8.1	1.0 1.0	10.9
23	43700	N.D. N.D. 0.9	N.D. N.D. 1.2	N.D.	49.6
27a	48 300	1.5 2.3 2.6	1.5 2.8 8.6	0.4 2.6	7.9
40b	4050	1.0 1.3 1.2	2.7 1.9 1.8	N.D.	9.8
40c	3760	0.6 7.2 6.7	0.8 5.9 18.7	0.3 0.6	14.5
40d	2400	1.2 1.3 1.3	1.3 1.9 2.6	0.3 1.2	7.3

^aN.D. = not determined. Fold-change over basal (1) = mean fold change versus control vehicle-treated cultures, with values greater than 1 indicating the induction of acetylation/phosphorylation.

METHODS

Chemistry: General Procedure. Unless otherwise noted, all reagents and solvents were of the highest commercial quality and used without further purification. All experiments dealing with moisture sensitive compounds were conducted under N₂. The reactions were monitored by thin layer chromatography (TLC) on silica gel-coated plates (Merck 60 F254) using reagent grade solvents. Flash column chromatography was performed on silica gel, particle size 60 Å, mesh = 230–400 (Merck) under standard techniques. Automated flash column chromatography was performed using ready-to-connect cartridges from Varian, on irregular silica gel, particle size 15–40 µm (normal phase disposable flash columns) on a Biotage SPX flash purification system. Microwave-assisted reactions were performed in a Biotage Smith Synthesis microwave reactor. The NMR spectroscopic data were recorded on a Bruker AV400 or VARIAN 400MR spectrometer with standard pulse sequences, operating at 400 MHz. Chemical shifts (δ) are reported in parts per million (ppm) downfield from tetramethylsilane (TMS), which was used as internal standard.

The abbreviations used to explain multiplicities are s = singlet, d = doublet, t = triplet, m = multiplet. Coupling constants (J) are in hertz. HPLC-analysis was performed using a Shimadzu LC-20AB or LC-20AD instrument with a Luna-C18(2), 5 µm, 2.0 × 50 mm column at 40 °C and UV detection at 215, 220, and 254 nm. Flow from the column was split to a MS spectrometer. The MS detector (Agilent 1200, 6110MS or Agilent 1200, 6120MS Quadrupole) was configured with an electrospray source or API/APCI. N₂ was used as the nebulizer gas. The source temperature was maintained at 50 °C. Data acquisition was accomplished with ChemStation LC/MSD quad software. All tested compounds possessed a purity of at least 95% established by HPLC, unless otherwise noted. Reported yields were not optimized, with the emphasis being on purity of product rather than quantity.

4-Ethoxy-3-(5-methyl-4-oxo-7-propyl-3H-imidazo[5,1-f][1,2,4]triazin-2-yl)benzenesulfonyl chloride (9). Commercially available 2-(2-ethoxyphenyl)-5-methyl-7-propyl-3H-imidazo[5,1-f][1,2,4]triazin-4(3H)-one (8) (0.5 g, 1.60 mmol) was added into ClSO₃H (10 mL) in ice–water and stirred at room temperature for 2 h. Then, the

Table 5. Comparison between Compounds 22 and 7 in Terms of Functional, Cellular, ADME, Toxicity, and Brain Permeability

	22	7 ¹⁷
in vitro efficacy in Tg2576 neurons		
AcH3K9 (increase, ^a 2 h)	0% (100 nM) 300% (500 nM)	50% (100 nM)
AcTub (increase, ^a 2 h)	50% (100 nM)	40% (100 nM)
pCREB (increase, ^a 2 h)	0% (100 nM) 100% (500 nM)	50% (100 nM)
hAPP processing (reduction, ^a 72 h)	25% (100 nM) 48% (500 nM)	50% (100 nM)
pTau (reduction ^a , 72 h)	0% (100 nM) 11% (500 nM)	50% (100 nM)
ADME		
solubility (at pH = 7.4)	7.84 µg/mL	29.8 µg/mL
PAMPA permeability (nm/s)	10.9	15.7
P450s inhibition: 1A2, 2C19, 2C9, 2D6, 3A4	<50% at 10 µM, except 3A4 (97.1%)	<50% at 10 µM, except 3A4 (75.2%)
liver microsomal stability, est <i>t</i> _{1/2} (min)	25.1 (human) 1.8 (mouse)	40.1 (human) 3.3 (mouse)
plasma protein binding, % unbound	1.9% (human) N.C. (mouse) ^b	1.8% (human) N.C. (mouse) ^b
toxicity		
THLE-2 (72 h)	LC ₅₀ : 9.4 µM (23.9 µM at 24 h)	LC ₅₀ : 7.2 µM (>100 µM at 24 h)
neurons (72 h)	LC ₅₀ : 6.1 µM	LC ₅₀ : 17.7 µM
PBMC (72 h)	LC ₅₀ : 6.2 µM	LC ₅₀ : 72.6 µM
brain tissue/plasma ratio (40 mg/kg; i.p.) ^c	brain concentration (nmol/kg): 255 plasma concentration (nM): 21252 log BB: -1.9 ratio: 1.2%	brain concentration (nmol/kg): 248 plasma concentration (nM): 18465 log BB: -1.87 ratio: 1.4%
in vivo efficacy (mice), by measuring a functional mark in hippocampus		
pCREB (40 mg/kg; i.p.)	0% increase at 15 min 0% increase at 30 min 25% increase at 60 min	148% increase at 30 min

^aOver nontreated. ^bN.C. = not calculable in mouse, unstable. ^cDetermined at *t* = 15 min for compound 22 (*n* = 3) and *t*_{max} for 7 (*n* = 4).

reaction mixture was quenched by adding water and filtered. The filtrate cake was collected and dried under vacuum to give the desired compound 9 (0.42 g, 64%). ESI-MS *m/z* 411 [M + H]⁺ calcd for C₁₇H₁₉ClN₄O₄S. ¹H NMR (CDCl₃, 400 MHz): *δ* 10.07 (s, 1H), 8.71–8.70 (d, *J* = 2.4 Hz, 1H), 8.20 (m, 1H), 7.20 (m, 1H), 4.41 (q, 2H), 3.15 (m, 2H), 2.72 (s, 3H), 1.85 (m, 2H), 1.50 (t, 3H), 0.99 (t, 3H).

Ethyl 4-[4-Ethoxy-3-(5-methyl-4-oxo-7-propyl-3H-imidazo[5,1-f]-[1,2,4]triazin-2-yl)phenyl]sulfonylpiperazin-1-yl]butanoate (10a). To a solution of compound 9 (0.62 g, 1.5 mmol) in EtOH (15 mL) was added ethyl 4-piperazin-1-ylbutanoate (**Int. 1**) (see synthesis in the Supporting Information) 0.3 g, 1.5 mmol) and Et₃N (303 mg, 3 mmol) and the reaction mixture was stirred at 100 °C under MW for 1 h. Then, the reaction mixture was concentrated under vacuum and partitioned with EtOAc and water. The organic phase was concentrated to give the desired compound 10a (0.6 g, 70%). ESI-MS *m/z* 575 [M + H]⁺ calcd for C₂₇H₃₈N₆O₆S. This intermediate was used in the next step without further characterization.

4-[4-Ethoxy-3-(5-methyl-4-oxo-7-propyl-3H-imidazo[5,1-f]-[1,2,4]triazin-2-yl)phenyl]sulfonylpiperazin-1-yl]butanoic acid (11a). To a solution of compound 10a (0.7 g, 1.22 mmol) in THF/MeOH/H₂O (10:1:5, 16 mL) was added LiOH·H₂O (270 mg, 6.4 mmol) and the resulting mixture was stirred at room temperature overnight. Then, the mixture was diluted with water and adjusted pH to 2–3 with 1 N HCl. Then, the solution was extracted with EtOAc and the organic phase was collected, dried over anhydrous Na₂SO₄, filtered, and concentrated to give compound 11a (0.5 g, 75%). ESI-MS *m/z* 547 [M + H]⁺ calcd for C₂₅H₃₄N₆O₆S. This intermediate was used in the next step without further characterization.

4-[4-Ethoxy-3-(5-methyl-4-oxo-7-propyl-3H-imidazo[5,1-f]-[1,2,4]triazin-2-yl)phenyl]sulfonylpiperazin-1-yl]butanamide (12a). To a solution of compound 11a (1050 mg, 1.92 mmol) in DMF (10 mL) was added EDC·HCl (737 mg, 3.84 mmol), HOBr (518 mg, 3.84 mmol), THPONH₂ (439 mg, 3.75 mmol) and NMM (582 mg, 5.76 mmol) and the mixture was stirred at room temperature overnight. Then, the mixture was diluted with EtOAc and the organic layer was washed with brine, dried over anhydrous Na₂SO₄, filtered, and concentrated to give the crude product which was purified by column chromatography to obtain compound 12a (0.7 g, 56%). ESI-MS *m/z* 646 [M + H]⁺ calcd for C₃₀H₄₃N₇O₇S. This intermediate was used in the next step without further characterization.

4-[4-Ethoxy-3-(5-methyl-4-oxo-7-propyl-3H-imidazo[5,1-f]-[1,2,4]triazin-2-yl)phenyl]sulfonylpiperazin-1-yl]butanehydroxamic acid (13a). A solution of compound 12a (50 mg, 0.077 mmol) in HCl/1,4-dioxane (4.0 M, 5 mL) was stirred at room temperature for 3 h. Then, the reaction mixture was concentrated to give the crude compound which was purified by preparative HPLC (method 7 described in the Supporting Information) to afford desired compound 13a (15 mg, 35%). ESI-MS *m/z* 562.1 [M + H]⁺ calcd for C₂₅H₃₅N₇O₆S. ¹H NMR (DMSO, 400 MHz): *δ* 11.85 (s, 1H), 10.51 (s, 1H), 9.67 (s, 1H), 7.91 (m, 2H), 7.49 (m, 1H), 4.15 (q, 2H), 3.15 (m, 8H), 2.78 (m, 2H), 2.61 (s, 3H), 2.35 (m, 2H), 1.98 (m, 2H), 1.75 (m, 4H), 1.35 (t, 3H), 0.99 (t, 3H).

Ethyl 2-[4-Ethoxy-3-(5-methyl-4-oxo-7-propyl-3H-imidazo[5,1-f]-[1,2,4]triazin-2-yl)phenyl]sulfonylpiperazin-1-yl]pyrimidine-5-carboxylate (10b). To a solution of 9 (410 mg, 1 mmol) in EtOH (15 mL) was added ethyl 2-piperazin-1-ylpyrimidine-5-carboxylate (**Int. 2**, see synthesis in the Supporting Information) (0.236 g, 1.0 mmol) and

Et_3N (303 mg, 3 mmol), and the reaction mixture was stirred at 100 °C under MW for 1 h. Then, the reaction mixture was concentrated under vacuum to give the desired compound **10b** (0.4 g, 66%). ESI-MS m/z 611 [M + H]⁺ calcd for $\text{C}_{28}\text{H}_{34}\text{N}_8\text{O}_6\text{S}$. This intermediate was used in the next step without further characterization.

2-[4-[4-Ethoxy-3-(5-methyl-4-oxo-7-propyl-3H-imidazo[5,1-f]-[1,2,4]triazin-2-yl)phenyl]sulfonylpiperazin-1-yl]pyrimidine-5-carboxylic acid (11b). To a solution of compound **10b** (0.4 g, 0.656 mmol) in THF/MeOH/H₂O (10:1:5, 16 mL) was added LiOH·H₂O (151 mg, 3.60 mmol) and the resulting mixture was stirred at room temperature overnight. Then, the mixture was diluted with water and adjusted pH to 2–3 with 1 N HCl. Then, the solution was extracted with EtOAc and the organic phase was collected, dried over anhydrous Na_2SO_4 , filtered, and concentrated to give compound **11b** (0.3 g, 78%). ESI-MS m/z 583 [M + H]⁺ calcd for $\text{C}_{26}\text{H}_{30}\text{N}_8\text{O}_6\text{S}$. This intermediate was used in the next step without further characterization.

2-[4-[4-Ethoxy-3-(5-methyl-4-oxo-7-propyl-3H-imidazo[5,1-f]-[1,2,4]triazin-2-yl)phenyl]sulfonylpiperazin-1-yl]-N-tetrahydropyran-2-yloxy-pyrimidine-5-carboxamide (12b). To a solution of compound **11b** (0.25 g, 0.43 mmol) in DMF (20 mL) was added EDC·HCl (100 mg, 0.52 mmol), HOBr (70 mg, 0.52 mmol), THPONH₂ (99 mg, 0.84 mmol) and NMM (214 mg, 2.15 mmol) and the mixture was stirred at room temperature overnight. Then, the mixture was diluted with EtOAc and the organic layer was washed with brine, dried over anhydrous Na_2SO_4 , filtered, and concentrated to give the crude product which was purified by column chromatography to obtain compound **12b** (150 mg, 51%). ESI-MS m/z 682 [M + H]⁺ calcd for $\text{C}_{31}\text{H}_{39}\text{N}_9\text{O}_5\text{S}$. This intermediate was used in the next step without further characterization.

2-[4-[4-Ethoxy-3-(5-methyl-4-oxo-7-propyl-3H-imidazo[5,1-f]-[1,2,4]triazin-2-yl)phenyl]sulfonylpiperazin-1-yl]pyrimidine-5-carbohydroxamic acid (13b). A solution of compound **12b** (150 mg, 0.22 mmol) in HCl/1,4-dioxane (2.0 M, 10 mL) was stirred at room temperature for 3 h. Then, the reaction mixture was concentrated to give the crude compound which was purified by preparative HPLC (method 8 described in the Supporting Information) to afford desired compound **13b** (40 mg, 30%). ESI-MS m/z 598.1 [M + H]⁺ calcd for $\text{C}_{26}\text{H}_{31}\text{N}_9\text{O}_6\text{S}$. ¹H NMR (DMSO, 400 MHz): δ 11.75 (s, 1H), 11.07 (s, 1H), 8.63 (s, 2H), 7.88 (m, 2H), 7.35 (m, 1H), 4.19 (q, 2H), 3.89 (m, 4H), 2.98 (m, 4H), 2.67 (m, 2H), 2.49 (s, 3H), 1.72 (m, 2H), 1.28 (t, 3H), 0.88 (t, 3H).

Ethyl (E)-3-[4-[4-[4-Ethoxy-3-(5-methyl-4-oxo-7-propyl-3H-imidazo[5,1-f][1,2,4]triazin-2-yl)phenyl]sulfonylpiperazin-1-yl]-methyl]phenyl]prop-2-enoate (10c). To a solution of compound **9** (0.62 g, 1.5 mmol) in EtOH (15 mL) was added ethyl (E)-3-[4-(piperazin-1-ylmethyl)phenyl]prop-2-enoate (Int. 3, see synthesis in Supporting Information) (0.45 g, 1.64 mmol) and Et_3N (303 mg, 3 mmol) and the reaction mixture was stirred at 100 °C under MW for 1 h. Then, the reaction mixture was concentrated under vacuum to give compound **10c** (0.8 g, 82%). ESI-MS m/z 649 [M + H]⁺ calcd for $\text{C}_{33}\text{H}_{40}\text{N}_6\text{O}_6\text{S}$. This intermediate was used in the next step without further characterization.

(E)-3-[4-[4-[4-Ethoxy-3-(5-methyl-4-oxo-7-propyl-3H-imidazo[5,1-f][1,2,4]triazin-2-yl)phenyl]sulfonylpiperazin-1-yl]methyl]phenyl]prop-2-enic acid (11c). To a solution of compound **10c** (0.9 g, 1.38 mmol) in THF/MeOH/H₂O (10:1:5, 16 mL) was added LiOH·H₂O (290 mg, 6.92 mmol) and the resulting mixture was stirred at room temperature overnight. Then, the mixture was diluted with water and adjusted pH to 2–3 with 1 N HCl. The resulting solution was extracted with EtOAc and the organic phases were collected, washed with brine, dried over anhydrous Na_2SO_4 , filtered, and concentrated to give compound **11c** (0.7 g, 82%). ESI-MS m/z 621 [M + H]⁺ calcd for $\text{C}_{31}\text{H}_{36}\text{N}_6\text{O}_6\text{S}$. This intermediate was used in the next step without further characterization.

(E)-3-[4-[4-[4-Ethoxy-3-(5-methyl-4-oxo-7-propyl-3H-imidazo[5,1-f][1,2,4]triazin-2-yl)phenyl]sulfonylpiperazin-1-yl]methyl]phenyl]-N-tetrahydropyran-2-yloxy-prop-2-enamide (12c). To a solution of compound **11c** (1.2 g, 1.94 mmol) in DMF (50 mL) was added EDC·HCl (740 mg, 3.84 mmol), HOBr (520 mg, 3.84 mmol), THPONH₂ (440 mg, 3.76 mmol) and NMM (590 mg, 5.76 mmol) and the mixture was stirred at room temperature overnight.

Then, the mixture was diluted with EtOAc and the organic layer was washed with brine, dried over anhydrous Na_2SO_4 , filtered, and concentrated to give the crude product which was purified by column chromatography to obtain compound **12c** (600 mg, 43%). ESI-MS m/z 720 [M + H]⁺ calcd for $\text{C}_{36}\text{H}_{45}\text{N}_7\text{O}_5\text{S}$. This intermediate was used in the next step without further characterization.

(E)-3-[4-[4-Ethoxy-3-(5-methyl-4-oxo-7-propyl-3H-imidazo[5,1-f][1,2,4]triazin-2-yl)phenyl]sulfonylpiperazin-1-yl]methyl]phenyl]prop-2-enehydroxamic acid (13c). A solution of compound **12c** (250 mg, 0.35 mmol) in HCl/1,4-dioxane (4.0 M, 10 mL) was stirred at room temperature for 3 h. Then, the reaction mixture was concentrated to give the crude compound which was purified by preparative TLC to obtain pure compound **13c** (51 mg, 23%). ESI-MS m/z 636.3 [M + H]⁺ calcd for $\text{C}_{31}\text{H}_{37}\text{N}_7\text{O}_6\text{S}$. ¹H NMR (DMSO, 400 MHz): δ 11.68 (m, 1H), 10.98 (m, 1H), 9.04 (m, 1H), 7.82 (m, 2H), 7.45–7.37 (m, 4H), 7.23 (m, 2H), 6.50 (d, J = 16 Hz, 1H), 4.19 (q, 2H), 3.45 (s, 2H), 2.95–2.65 (m, 6H), 2.47 (s, 3H), 2.41 (m, 4H), 1.69 (m, 2H), 1.32 (m, 3H), 0.88 (t, 3H).

Ethyl (E)-3-[4-[4-ethoxy-3-(5-methyl-4-oxo-7-propyl-3H-imidazo[5,1-f][1,2,4]triazin-2-yl)phenyl]sulfonylaminophenyl]prop-2-enoate (10d). To a solution of **9** (0.41 g, 1.0 mmol) in pyridine (10 mL) was added ethyl (E)-3-(4-aminophenyl)prop-2-enoate (Int. 4, see synthesis in the Supporting Information) (0.19 g, 1.0 mmol) and the reaction mixture was stirred at room temperature overnight. Then, the reaction mixture was concentrated under vacuum and the residue was washed with water and extracted with CH₂Cl₂. The organic phase was dried over Na_2SO_4 , filtered, and concentrated to give the desired compound **10d** (0.4 g, 71%). ESI-MS m/z 566 [M + H]⁺ calcd for $\text{C}_{28}\text{H}_{31}\text{N}_5\text{O}_6\text{S}$. This intermediate was used in the next step without further characterization.

(E)-3-[4-[4-Ethoxy-3-(5-methyl-4-oxo-7-propyl-3H-imidazo[5,1-f][1,2,4]triazin-2-yl)phenyl]sulfonylaminophenyl]prop-2-enoic acid (11d). To a solution of compound **10d** (1.5 g, 2.65 mmol) in THF/MeOH/H₂O (10:1:5, 16 mL) was added LiOH·H₂O (560 mg, 13.25 mmol) and the resulting mixture was stirred at room temperature overnight. Then, the mixture was diluted with water and adjusted pH to 2–3 with 1 N HCl. The resulting solution was extracted with EtOAc and the organic phases were collected, washed with brine, dried over anhydrous Na_2SO_4 , filtered, and concentrated to give compound **11d** (1.0 g, 70%). ESI-MS m/z 538 [M + H]⁺ calcd for $\text{C}_{26}\text{H}_{27}\text{N}_5\text{O}_6\text{S}$. This intermediate was used in the next step without further characterization.

(E)-3-[4-[4-Ethoxy-3-(5-methyl-4-oxo-7-propyl-3H-imidazo[5,1-f][1,2,4]triazin-2-yl)phenyl]sulfonylaminophenyl]prop-2-enoic acid (11d). To a solution of compound **11d** (0.3 g, 0.56 mmol) in DMF (10 mL) was added EDC·HCl (129 mg, 0.67 mmol), HOBr (90 mg, 0.67 mmol), THPONH₂ (128 mg, 1.1 mmol) and NMM (282 mg, 2.79 mmol) and the mixture was stirred at room temperature overnight. Then, the mixture was diluted with EtOAc and the organic layer was washed with brine, dried over anhydrous Na_2SO_4 , filtered, and concentrated to give the crude product which was purified by column chromatography to obtain compound **12d** (0.3 g, 84%). ESI-MS m/z 637 [M + H]⁺ calcd for $\text{C}_{31}\text{H}_{36}\text{N}_6\text{O}_5\text{S}$. This intermediate was used in the next step without further characterization.

(E)-3-[4-[4-Ethoxy-3-(5-methyl-4-oxo-7-propyl-3H-imidazo[5,1-f][1,2,4]triazin-2-yl)phenyl]sulfonylaminophenyl]prop-2-enehydroxamic acid (13d). A solution of compound **12d** (150 mg, 0.24 mmol) in HCl/1,4-dioxane (4.0 M, 10 mL) was stirred at room temperature for 3 h. Then, the reaction mixture was concentrated to give the crude compound which was purified by preparative HPLC (method 6 described in the Supporting Information) to obtain compound **13d** (102 mg, 77%). ESI-MS m/z 553.1 [M + H]⁺ calcd for $\text{C}_{26}\text{H}_{28}\text{N}_6\text{O}_6\text{S}$. ¹H NMR (DMSO, 400 MHz): δ 11.95 (s, 1H), 10.56 (s, 1H), 7.94 (m, 2H), 7.45–7.40 (m, 2H), 7.39–7.31 (m, 2H), 7.25–7.15 (m, 2H), 6.32 (d, J = 16 Hz, 1H), 4.17 (q, 2H), 2.90 (m, 2H), 2.54 (s, 3H), 1.77 (m, 2H), 1.30 (t, 3H), 0.99 (t, 3H).

2-(2-Ethoxy-5-iodo-phenyl)-5-methyl-7-propyl-3H-imidazo[5,1-f][1,2,4]triazin-4(3H)-one (14). To a solution of commercially available 2-(2-ethoxyphenyl)-5-methyl-7-propyl-3H-imidazo[5,1-f][1,2,4]triazin-4(3H)-one (**8**) (5 g, 16 mmol) in TFA (50 mL) was

added NIS (4.3 g, 19.2 mmol) at 0 °C and the mixture was stirred at room temperature overnight. Then, the mixture was quenched with water and extracted with EtOAc. The organic layer was washed with brine, dried over anhydrous Na₂SO₄, filtered, and concentrated to give the crude product which was purified by column chromatography to obtain compound 14 (5 g, 71%) as a white solid. ESI-MS *m/z* 439.1 [M + H]⁺ calcd for C₁₇H₁₉IN₄O₂. This intermediate was used in the next step without further characterization.

2-[2-Ethoxy-5-(4,4,5,5-tetramethyl-1,3,2-dioxaborolan-2-yl)-phenyl]-5-methyl-7-propyl-3H-imidazo[5,1-f][1,2,4]triazin-4(3H)-one (15). To a solution of compound 14 (5.5 g, 12.56 mmol) in 1,4-dioxane (30 mL) was added 4,4,5,5-tetramethyl-2-(4,4,5,5-tetramethyl-1,3,2-dioxaborolan-2-yl)-1,3,2-dioxaborolane (3.84 g, 15.12 mmol), Pd(dppf)Cl₂ (2.6 g, 3.56 mmol) and KOAc (3.69 g, 37.7 mmol) and the mixture was stirred at 90 °C overnight. Then, the mixture was quenched with water and extracted with EtOAc. The organic layer was washed with brine, dried over anhydrous Na₂SO₄, filtered, and concentrated to give the crude product which was purified by column chromatography to obtain compound 15 (3.5 g, 64%) as a white solid. ESI-MS *m/z* 439.1 [M + H]⁺ calcd for C₂₃H₃₁N₄O₄. This intermediate was used in the next step without further characterization.

Methyl (E)-3-[4-[4-Ethoxy-3-(5-methyl-4-oxo-7-propyl-3H-imidazo[5,1-f][1,2,4]triazin-2-yl)phenyl]methyl]phenyl]prop-2-enoate (16). To a solution of compound 15 (300 mg, 0.685 mmol) in 1,4-dioxane/H₂O (5:2, 7 mL) was added methyl (E)-3-[4-(bromomethyl)phenyl]prop-2-enoate (190 mg, 0.75 mmol), Pd(PPh₃)₄ (79 mg, 0.068 mmol) and K₂CO₃ (284 mg, 2.06 mmol) and the mixture was stirred at 85 °C for 1 h under MW. Then, the mixture was quenched with water and extracted with EtOAc. The organic layer was washed with brine, dried over anhydrous Na₂SO₄, filtered, and concentrated to give the crude product which was purified by column chromatography to afford pure compound 16 (150 mg, 45%) as a white solid. ESI-MS *m/z* 487.2 [M + H]⁺ calcd for C₂₈H₃₀N₄O₄. This intermediate was used in the next step without further characterization.

(E)-3-[4-[4-Ethoxy-3-(5-methyl-4-oxo-7-propyl-3H-imidazo[5,1-f][1,2,4]triazin-2-yl)phenyl]methyl]phenyl]prop-2-enoic acid (17). To a solution of compound 16 (150 mg, 0.31 mmol) in THF/MeOH/H₂O (3:3:2, 16 mL) was added LiOH·H₂O (130 mg, 3.1 mmol) and the resulting mixture was stirred at room temperature overnight. Then, the mixture was diluted with water and adjusted pH to 6–7 with 1 N HCl. The mixture was extracted with EtOAc and the organic layer was washed with brine, dried over anhydrous Na₂SO₄, filtered, and concentrated to afford the desired product 17 (120 mg, 82%). ESI-MS *m/z* 473.2 [M + H]⁺ calcd for C₂₇H₂₈N₄O₄. This intermediate was used in the next step without further characterization.

(E)-3-[4-[4-Ethoxy-3-(5-methyl-4-oxo-7-propyl-3H-imidazo[5,1-f][1,2,4]triazin-2-yl)phenyl]methyl]phenyl]-N-tetrahydropyran-2-yloxy-prop-2-enamide (18). To a solution of compound 17 (140 mg, 0.3 mmol) in DMF (10 mL) was added EDC·HCl (120 mg, 0.6 mmol), HOBT (80 mg, 0.6 mmol), THPONH₂ (60 mg, 0.5 mmol) and NMM (100 mg, 0.9 mmol) and the mixture was stirred at room temperature overnight. Then, the mixture was quenched with water and extracted with EtOAc. The organic layer was washed with brine, dried over anhydrous Na₂SO₄, filtered, and concentrated to give the crude product which was purified by preparative TLC to obtain compound 18 (70 mg, 41%) as a pale yellow solid. ESI-MS *m/z* 572.2 [M + H]⁺ calcd for C₃₂H₃₇N₅O₅. This intermediate was used in the next step without further characterization.

(E)-3-[4-[4-Ethoxy-3-(5-methyl-4-oxo-7-propyl-3H-imidazo[5,1-f][1,2,4]triazin-2-yl)phenyl]methyl]phenyl]prop-2-enehydroxamic acid (19). A solution of compound 18 (70 mg, 0.12 mmol) in HCl/EtOAc (2.0 M, 10 mL) was stirred at room temperature for 1 h. Then, the mixture was concentrated to give the crude product which was purified by preparative HPLC (method 9 described in the Supporting Information) to obtain pure compound 19 (5.3 mg, 10%) as a white solid. ESI-MS *m/z* 488.1 [M + H]⁺ calcd for C₂₇H₂₉N₅O₄. ¹H NMR (MeOD, 400 MHz): δ 7.60–7.45 (m, 4H), 7.45–7.40 (m, 1H), 7.30–7.20 (m, 2H), 7.15–7.05 (m, 1H), 6.45–6.35 (m, 1H), 4.20–4.15 (m, 2H), 4.02 (s, 2H), 3.05–2.95 (m, 2H), 2.64 (s, 3H), 1.86–1.80 (m, 2H), 1.44–1.40 (m, 3H), 1.00–0.97 (m, 3H).

Ethyl 3-[4-Ethoxy-3-(5-methyl-4-oxo-7-propyl-3H-imidazo[5,1-f][1,2,4]triazin-2-yl)phenyl]methyl]cyclobutanecarboxylate (20). Compound 14 (0.6 g, 1.37 mmol) was dissolved in 1,4-dioxane/H₂O (5:1, 24 mL) and Pd₂(dba)₃ (120 mg, 0.14 mmol), xantphos (66 mg, 0.11 mmol) and Na₂CO₃ (454 mg, 4.2 mmol) were added. Then, freshly prepared ethyl 3-(9-borabicyclo[3.3.1]nonan-9-ylmethyl)cyclobutanecarboxylate (Int. 5, see synthesis in the Supporting Information) (1.43 mmol in 10 mL of THF) was added and the mixture was stirred at reflux overnight. Then, the solution was filtered and the filtrate was extracted with EtOAc. The organic layer was washed with brine, dried over anhydrous Na₂SO₄, filtered, and concentrated to give the crude compound which was purified by column chromatography to afford pure compound 20 (200 mg, 33%) as a pale yellow oil. ESI-MS *m/z* 453.2 [M + H]⁺ calcd for C₂₅H₃₂N₄O₄. This intermediate was used in the next step without further characterization.

3-[4-Ethoxy-3-(5-methyl-4-oxo-7-propyl-3H-imidazo[5,1-f][1,2,4]triazin-2-yl)phenyl]methyl]cyclobutanecarboxylic acid (21). To a solution of compound 20 (200 mg, 0.44 mmol) in THF/MeOH/H₂O (3:3:2, 16 mL) was added LiOH·H₂O (184 mg, 4.4 mmol) and the resulting mixture was stirred at room temperature overnight. Then, the mixture was diluted with water, adjusted pH to 6–7 with 1 N HCl and the solution was extracted with EtOAc. The organic layer was washed with brine, dried over anhydrous Na₂SO₄, filtered, and concentrated to afford the desired compound 21 (160 mg, 85%). ESI-MS *m/z* 425.2 [M + H]⁺ calcd for C₂₃H₂₈N₄O₄. This intermediate was used in the next step without further characterization.

3-[4-Ethoxy-3-(5-methyl-4-oxo-7-propyl-3H-imidazo[5,1-f][1,2,4]triazin-2-yl)phenyl]methyl]cyclobutanecarboxylic acid (22). To a solution of compound 21 (160 mg, 0.38 mmol) in DMF (10 mL) was added NH₂OH·HCl (529 mg, 7.6 mmol), DIEA (491 mg, 3.8 mmol) and BOP (335 mg, 0.76 mmol) and the mixture was stirred at room temperature overnight. Then, the mixture was quenched with water and extracted with EtOAc. The organic layer was washed with brine, dried over anhydrous Na₂SO₄, filtered, and concentrated to give the crude product which was purified by preparative HPLC (method 9 described in the Supporting Information) to afford compound 22 (58.4 mg, 35%) as a pale yellow solid. ESI-MS *m/z* 440.2 [M + H]⁺ calcd for C₂₃H₂₉N₅O₄. ¹H NMR (MeOD, 400 MHz): δ 7.52 (s, 1H), 7.40–7.37 (m, 1H), 7.11–7.09 (m, 1H), 4.20–4.14 (m, 2H), 3.18–3.14 (m, 2H), 2.80–2.75 (m, 1H), 2.75–2.71 (m, 5H), 2.60–2.45 (m, 1H), 2.40–2.25 (m, 1H), 2.25–2.10 (m, 1H), 2.05–1.85 (m, 4H), 1.44–1.41 (m, 3H), 1.10–1.04 (m, 3H). ¹³C NMR (DMSO-d₆, 400 MHz): δ 14.4 (CH₃), 15.4 (CH₃), 20.7, 27.0, 30.0, 31.4, 31.6, 33.0, 33.3, 33.8, 64.9 (CH₂O), 113.7, 115.2, 119.9, 130.8, 131.0, 133.1, 133.4, 143.9, 150.6 (C=O), 155.4, 155.9, 171.4 (CONHOH).

3-[4-Ethoxy-3-(5-methyl-4-oxo-7-propyl-3H-imidazo[5,1-f][1,2,4]triazin-2-yl)phenyl]methyl]N-methoxy-N-methyl-cyclobutanecarboxamide (23). To a solution of compound 21 (500 mg, 1.17 mmol) in DMF (10 mL) was added EDC·HCl (461 mg, 2.4 mmol), HOBT (324 mg, 2.4 mmol), N,O-dimethylhydroxylamine (146 mg, 2.4 mmol) and NMM (363 mg, 3.6 mmol) and the mixture was stirred at room temperature overnight. Then, the reaction was quenched with water and extracted with EtOAc. The organic layer was washed with brine, dried over anhydrous Na₂SO₄, filtered, and concentrated to give the crude product which was purified by preparative TLC to obtain compound 23 (17 mg, 3%) as a pale yellow solid. ESI-MS *m/z* 468.2 [M + H]⁺ calcd for C₂₅H₃₃N₅O₄. ¹H NMR (MeOD, 400 MHz): δ 7.55–7.50 (m, 1H), 7.50–7.35 (m, 1H), 7.15–7.05 (m, 1H), 4.25–4.10 (m, 2H), 3.70–3.60 (m, 3H), 3.50–3.00 (m, 5H), 2.85–2.75 (m, 1H), 2.75–2.40 (m, 6H), 2.40–2.10 (m, 2H), 2.10–1.80 (m, 4H), 1.40–1.25 (m, 3H), 1.10–0.90 (m, 3H).

Ethyl 4-[4-Ethoxy-3-(5-methyl-4-oxo-7-propyl-3H-imidazo[5,1-f][1,2,4]triazin-2-yl)phenyl]cyclohexanecarboxylate (24). To a solution of compound 15 (876 mg, 2.0 mmol) in 1,4-dioxane/H₂O (6:1, 70 mL) was added ethyl 4-(trifluoromethylsulfonyloxy)cyclohex-3-ene-1-carboxylate (906 mg, 3.0 mmol), K₂CO₃ (1.04 g, 7.5 mmol), and Pd(PPh₃)₄ (346 mg, 0.3 mmol), and the mixture was stirred at 80 °C overnight under N₂ protection. Then, the mixture was extracted

with EtOAc and the organic layer was washed with brine, dried over anhydrous Na_2SO_4 , filtered and concentrated to give a residue which was purified by column chromatography to obtain pure intermediate ethyl 4-[4-ethoxy-3-(5-methyl-4-oxo-7-propyl-3H-imidazo[5,1-f]-[1,2,4]triazin-2-yl)phenyl]cyclohex-3-ene-1-carboxylate (352 mg, 38%) as a yellow solid. ESI-MS m/z 465.2 [$\text{M} + \text{H}$]⁺ calcd for $\text{C}_{26}\text{H}_{32}\text{N}_4\text{O}_4$. To a solution of this intermediate (352 mg, 0.76 mmol) in EtOAc (40 mL) was added Pd/C (0.2 g) under H_2 (1 atm), and the mixture was stirred at room temperature for 3 h. Then, the mixture was filtered and the filtrate was concentrated to give compound 24 (320 mg, 90%) as yellow solid. ESI-MS m/z 467.2 [$\text{M} + \text{H}$]⁺ calcd for $\text{C}_{26}\text{H}_{34}\text{N}_4\text{O}_4$. This intermediate was used in the next step without further characterization.

4-[4-Ethoxy-3-(5-methyl-4-oxo-7-propyl-3H-imidazo[5,1-f]-[1,2,4]triazin-2-yl)phenyl]cyclohexanecarboxylic acid (25). To a solution of compound 24 (320 mg, 0.69 mmol) in MeOH/THF/ H_2O (1:3:1, 30 mL) was added LiOH· H_2O (295 mg, 7 mmol) and the reaction mixture was stirred at room temperature overnight. Then, the mixture was concentrated, diluted with H_2O , and adjusted pH to 1–2 with 1 N HCl. The solution was extracted with EtOAc and the organic layer was washed with brine, dried over anhydrous Na_2SO_4 , filtered, and concentrated to give compound 25 (307 mg, 99% crude). ESI-MS m/z 439 [$\text{M} + \text{H}$]⁺ calcd for $\text{C}_{24}\text{H}_{30}\text{N}_4\text{O}_4$. This intermediate was used in the next step without further characterization.

4-[4-Ethoxy-3-(5-methyl-4-oxo-7-propyl-3H-imidazo[5,1-f]-[1,2,4]triazin-2-yl)phenyl]-N-tetrahydropyran-2-yloxy-cyclohexane-carboxamide (26). To a solution of compound 25 (307 mg, 0.69 mmol) in DMF (30 mL) was added EDC·HCl (290 mg, 1.5 mmol), HOEt (203 mg, 1.5 mmol), THPONH₂ (176 mg, 1.5 mmol) and NMM (253 mg, 2.5 mmol) and the mixture was stirred at room temperature overnight. Then, the reaction was quenched with water and extracted with EtOAc. The organic layer was washed with brine, dried over anhydrous Na_2SO_4 , filtered, and concentrated to give the crude product which was purified by preparative TLC to obtain pure compound 26 (246 mg, 66%) as yellow solid. ESI-MS m/z 538.3 [$\text{M} + \text{H}$]⁺ calcd for $\text{C}_{29}\text{H}_{39}\text{N}_5\text{O}_5$. This intermediate was used in the next step without further characterization.

4-[4-Ethoxy-3-(5-methyl-4-oxo-7-propyl-3H-imidazo[5,1-f]-[1,2,4]triazin-2-yl)phenyl]cyclohexanecarbohydroxamic acid (27). A solution of compound 26 (246 mg, 0.46 mmol) in HCl/EtOAc (1.0 M, 20 mL) was stirred at room temperature for 1 h. Then, the mixture was concentrated to give the crude product which was purified by preparative HPLC (method 9 described in the *Supporting Information*) to obtain pure compound 27 (10.8 mg, 5%), 27a (18.5 mg, 9%) and 27b (24.8 mg, 12%). 27; ESI-MS m/z 454.2 [$\text{M} + \text{H}$]⁺ calcd for $\text{C}_{24}\text{H}_{31}\text{N}_5\text{O}_4$. ¹H NMR (MeOD, 400 MHz): δ 7.60–7.55 (m, 1H), 7.50–7.45 (m, 1H), 7.12 (d, $J = 8.4$ Hz, 1H), 4.20–4.15 (m, 2H), 3.18–3.15 (m, 2H), 2.77 (s, 3H), 2.44 (m, 1H), 2.14–1.88 (m, 7H), 1.73–1.68 (m, 4H), 1.41 (t, $J = 7.2$ Hz, 3H), 1.06 (t, $J = 7.6$ Hz, 3H). 27a; ESI-MS m/z 454.2 [$\text{M} + \text{H}$]⁺ calcd for $\text{C}_{24}\text{H}_{31}\text{N}_5\text{O}_4$. ¹H NMR (MeOD, 400 MHz): δ 7.56 (d, $J = 1.6$ Hz, 1H), 7.44 (d, $J = 8.4$ Hz, 1H), 7.11 (d, $J = 8.8$ Hz, 1H), 4.20–4.14 (m, 2H), 3.13–3.11 (m, 2H), 2.69 (s, 3H), 2.62–2.59 (m, 1H), 2.40–2.19 (m, 1H), 1.98–1.87 (m, 6H), 1.72–1.70 (m, 2H), 1.54 (m, 2H), 1.41 (t, $J = 7.2$ Hz, 3H), 1.05 (t, $J = 6.8$ Hz, 3H). 27b; ESI-MS m/z 454.2 [$\text{M} + \text{H}$]⁺ calcd for $\text{C}_{24}\text{H}_{31}\text{N}_5\text{O}_4$. ¹H NMR (MeOD, 400 MHz): δ 7.60 (s, 1H), 7.50–7.47 (m, 1H), 7.12 (d, $J = 8.8$ Hz, 1H), 4.20–4.15 (m, 2H), 3.17–3.14 (m, 2H), 2.76–2.71 (m, 4H), 2.44 (m, 1H), 2.04–2.00 (m, 4H), 1.91–1.88 (m, 2H), 1.76–1.70 (m, 4H), 1.41 (t, $J = 7.2$ Hz, 3H), 1.06 (t, $J = 7.6$ Hz, 3H).

1,3-Benzodioxole-5-carbaldehyde (29). A solution of commercially available 1,3-benzodioxole-5-ylmethanol (28) (100 g, 0.66 mol) and active MnO₂ (572 g, 6.6 mol) in CH₂Cl₂ (1000 mL) was stirred at room temperature overnight. Then, the reaction mixture was filtered and the filtrate was washed with brine, dried over anhydrous Na_2SO_4 , filtered, and concentrated to give compound 29 (80 g, 80%) as a white solid. ESI-MS m/z 151 [$\text{M} + \text{H}$]⁺ calcd for $\text{C}_8\text{H}_6\text{O}_3$. This intermediate was used in the next step without further characterization.

Methyl (1R,3R)-1-(1,3-Benzodioxol-5-yl)-2,3,4,9-tetrahydro-1H-pyrido[3,4-b]indole-3-carboxylate (30). A solution of compound 29

(30 g, 0.2 mol) and (R)-methyl 2-amino-3-(1H-indol-3-yl)propanoate (43.6 g, 0.2 mol) in propan-2-ol (500 mL) was refluxed overnight. Then, the reaction mixture was concentrated and the solid was dissolved in aqueous NaHCO₃ and CH₂Cl₂. The organic phase was separated, dried over Na_2SO_4 , filtered, and concentrated. The residue was stirred in a mixture of CH₂Cl₂ (50 mL) and hexane (600 mL). The resulting solid was filtered off and the filtration was concentrated to give compound 30 (50 g, 71% yield). ESI-MS m/z 351 [$\text{M} + \text{H}$]⁺ calcd for $\text{C}_{20}\text{H}_{18}\text{N}_2\text{O}_4$. ¹H NMR (CDCl₃, 400 MHz): δ 7.54–7.52 (m, 1H), 7.48 (s, 1H), 7.26–7.22 (m, 1H), 7.16–7.11 (m, 2H), 6.89–6.75 (m, 3H), 5.94 (s, 2H), 5.16 (s, 1H), 3.97–3.96 (m, 1H), 3.81 (s, 3H), 3.24–3.18 (m, 1H), 3.05–2.96 (m, 1H).

Methyl (1R,3R)-1-(1,3-Benzodioxol-5-yl)-2-(2-chloroacetyl)-1,3,4,9-tetrahydropyrido[3,4-b]indole-3-carboxylate (31). To a solution of compound 30 (50 g, 0.14 mol) and Et₃N (29 g, 0.28 mol) in anhydrous THF (500 mL) was added chloro-acetyl chloride (17.7 g, 0.16 mol) at 0 °C and the reaction mixture was stirred at room temperature for 3 h. Then, the mixture was diluted with CH₂Cl₂ (300 mL), washed with aqueous NaHCO₃, dried over Na_2SO_4 , filtered and concentrated to give compound 31 (20 g, 33%) as a yellow solid. ESI-MS m/z 427 [$\text{M} + \text{H}$]⁺ calcd for $\text{C}_{22}\text{H}_{19}\text{ClN}_2\text{O}_5$. This intermediate was used in the next step without further characterization.

6-(Benzodioxol-5-yl)-2,3,6,7,12,12a-hexahydropyrazino[1',2':1,6]pyrido[3,4-b]indole-1,4-dione (32). A solution of compound 31 (5 g, 11.7 mmol) in NH₃/MeOH (30 mL, 30%) was stirred at 40 °C for 3 days. Then, the reaction mixture was concentrated and the residue was dissolved in CH₂Cl₂ (50 mL), washed with water (50 mL × 3), dried over Na_2SO_4 , filtered, and concentrated to give compound 31 (3 g, 68%) as white solid. ESI-MS m/z 376 [$\text{M} + \text{H}$]⁺ calcd for $\text{C}_{21}\text{H}_{17}\text{N}_3\text{O}_4$. ¹H NMR (DMSO, 400 MHz): δ 11.07 (s, 1H), 8.36 (s, 1H), 7.55–7.53 (m, 1H), 7.32–7.30 (m, 1H), 7.08–6.96 (m, 2H), 6.86 (s, 1H), 6.86–6.75 (m, 2H), 6.17 (s, 1H), 5.93 (s, 2H), 4.42–4.36 (m, 1H), 4.06–4.02 (m, 1H), 3.75–3.70 (m, 1H), 3.47–3.42 (m, 1H), 2.98–2.91 (m, 1H).

Ethyl (E)-3-(4-(6-(Benzodioxol-5-yl)-1,4-dioxo-3,4,6,7,12,12a-hexahydropyrazino[1',2':1,6]pyrido[3,4-b]indol-2(1H)-yl)phenyl)acrylate (33). To a solution of compound 32 (0.6 g, 1.6 mmol) in 1,4-dioxane (15 mL) was added CuI (0.6 g, 3.2 mmol), K₃PO₄ (0.68 g, 3.2 mmol), (\pm)-trans-1,2-diaminocyclohexane (0.72 g, 6.4 mmol), and ethyl (E)-3-(4-iodophenyl)prop-2-enoate (Int. 6, see synthesis in the *Supporting Information*) (0.48 g, 1.6 mmol), and the reaction mixture was stirred at room temperature for 8 days. Then, the mixture was concentrated and extracted with EtOAc. The combined organic layers were washed with brine, dried over anhydrous Na_2SO_4 , filtered, and concentrated to give the crude product which was purified by column chromatography to obtain compound 33 (0.3 g, 34%) as a pale yellow solid. ESI-MS m/z 550 [$\text{M} + \text{H}$]⁺ calcd for $\text{C}_{32}\text{H}_{27}\text{N}_3\text{O}_6$. ¹H NMR (CDCl₃, 400 MHz): δ 7.99 (s, 1H), 7.66 (d, $J = 16$ Hz, 1H), 7.60–7.57 (m, 2H), 7.56–7.54 (m, 1H), 7.37–7.32 (m, 3H), 7.26–7.25 (m, 1H), 7.25–7.17 (m, 1H), 7.02 (s, 1H), 6.85 (s, 1H), 6.75 (s, 2H), 6.43 (d, $J = 16$ Hz, 1H), 5.95 (s, 2H), 4.56–4.54 (m, 1H), 4.37–4.24 (m, 2H), 4.02 (s, 1H), 3.60–3.57 (m, 1H), 3.15–3.11 (m, 1H), 1.36–1.32 (m, 3H).

(E)-3-(4-(6-(Benzodioxol-5-yl)-1,4-dioxo-3,4,6,7,12,12a-hexahydropyrazino[1',2':1,6]pyrido[3,4-b]indol-2(1H)-yl)phenyl)-N-hydroxyacrylamide (34). To a solution of compound 33 (100 mg, 0.18 mmol) in NH₂OH/MeOH (2.0 M, 3 mL) was added NaCN (1.7 mg, 0.036 mmol) and the reaction mixture was stirred at 50 °C for 3 h. Then, the mixture was concentrated and extracted with EtOAc. The combined organic layers were washed with brine, dried over anhydrous Na_2SO_4 , filtered, and concentrated to give the crude product which was purified by preparative HPLC (method 1 described in the *Supporting Information*) to afford compound 34 (5.6 mg, 6%) as a pale yellow solid. ESI-MS m/z 537.2 [$\text{M} + \text{H}$]⁺ calcd for $\text{C}_{30}\text{H}_{24}\text{N}_4\text{O}_6$. ¹H NMR (CD₃CN, 400 MHz): δ 9.13 (s, 1H), 7.59–7.57 (m, 1H), 7.52–7.50 (m, 1H), 7.40–7.36 (m, 3H), 7.20–7.16 (m, 1H), 7.14–7.08 (m, 1H), 6.97 (s, 1H), 6.89 (s, 1H), 6.82–6.81 (m, 1H), 6.79–6.74 (m, 1H), 5.98 (s, 2H), 5.00–4.98 (m, 1H), 4.57–4.53 (m, 1H), 4.42–4.41 (m, 1H), 4.39–4.38 (m, 1H), 3.46–3.41 (m, 1H), 3.21–3.11 (m, 2H), 2.93–2.91 (m, 1H).

tert-Butyl 4-(6-(Benzod[[1,3]dioxol-5-yl)-1,4-dioxo-3,4,6,7,12,12a-hexahdropyrazino[1',2':1,6]pyrido[3,4-b]indol-2(1H)-yl)piperidine-1-carboxylate (35a). To a solution of compound 31 (10.8 g, 0.025 mol) in MeOH (300 mL) was added *tert*-butyl 4-aminopiperidine-1-carboxylate (5.1 g, 0.025 mol) and the reaction mixture was stirred at 90 °C for 3 days. Then, the mixture was concentrated and extracted with EtOAc. The combined organic layers were washed with brine, dried over anhydrous Na₂SO₄, filtered, and concentrated to give the crude product which was purified by column chromatography to afford compound 35a (2.5 g, 18%) as a pale white solid. ESI-MS *m/z* 559 [M + H]⁺ calcd for C₃₁H₃₄N₄O₆. ¹H NMR (CDCl₃, 400 MHz): δ 8.08 (s, 1H), 7.61–7.60 (m, 1H), 7.28–7.26 (m, 1H), 7.19–7.15 (m, 2H), 6.80–6.79 (m, 1H), 6.70–6.65 (m, 1H), 6.18 (s, 1H), 5.85 (d, *J* = 6.8 Hz, 2H), 4.65–4.58 (m, 1H), 4.29–4.15 (m, 3H), 3.96–3.83 (m, 2H), 3.75–3.69 (m, 1H), 3.25–3.18 (m, 1H), 2.85–2.78 (m, 2H), 1.75–1.70 (m, 3H), 1.61–1.57 (m, 2H), 1.46 (s, 9H).

6-(Benzod[[1,3]dioxol-5-yl)-2-(piperidin-4-yl)-2,3,6,7,12,12a-hexahdropyrazino[1',2':1,6]pyrido[3,4-b]indole-1,4-dione (36a). To a solution of compound 35a (2.5 g, 4.4 mol) in CH₂Cl₂ (50 mL) was added TFA (1 mL), and the reaction mixture was stirred at room temperature for 2 h. Then, the mixture was concentrated to give compound 36a (2.4 g, 99% crude) as a yellow solid. ESI-MS *m/z* 459 [M + H]⁺ calcd for C₂₆H₂₆N₄O₄. This intermediate was used in the next step without further characterization.

Ethyl 4-(4-(6-(Benzod[[1,3]dioxol-5-yl)-1,4-dioxo-3,4,6,7,12,12a-hexahdropyrazino[1',2':1,6]pyrido[3,4-b]indol-2(1H)-yl)piperidin-1-yl)butanoate (37a). To a solution of compound 36a (0.4 g, 0.87 mmol) in CH₃CN (10 mL) was added ethyl 4-bromobutanoate (0.25 g, 1.31 mmol), K₂CO₃ (0.36 g, 2.61 mmol) and KI (0.029 g, 0.17 mmol) and the reaction mixture was stirred at room temperature for 12 h. Then, the mixture was concentrated to give the crude product which was purified by column chromatography to afford compound 37a (0.2 g, 41%) as a yellow solid. ESI-MS *m/z* 573 [M + H]⁺ calcd for C₃₂H₃₆N₄O₆. This intermediate was used in the next step without further characterization.

4-(4-(6-(Benzod[[1,3]dioxol-5-yl)-1,4-dioxo-3,4,6,7,12,12a-hexahdropyrazino[1',2':1,6]pyrido[3,4-b]indol-2(1H)-yl)piperidin-1-yl)-N-hydroxybutanamide (40a). To a solution of compound 37a (100 mg, 0.17 mmol) in NH₂OH/MeOH (2.0 M, 3 mL) was added NaCN (1.5 mg, 0.030 mmol), and the reaction mixture was stirred at 50 °C for 3 h. Then, the mixture was concentrated and extracted with EtOAc. The combined organic layers were washed with brine, dried over anhydrous Na₂SO₄, filtered, and concentrated to give the crude product which was purified by preparative HPLC (method 4 described in the Supporting Information) to afford compound 40a (11.6 mg, 12%) as a pale yellow solid. ESI-MS *m/z* 560.1 [M + H]⁺ calcd for C₃₀H₃₃N₅O₆. ¹H NMR (DMSO, 400 MHz): δ 11.08–11.04 (m, 1H), 10.51 (s, 1H), 9.35–9.31 (m, 1H), 7.51–7.40 (m, 1H), 7.31–7.29 (m, 1H), 7.10–6.95 (m, 2H), 6.88–6.62 (m, 3H), 6.16 (s, 1H), 6.01 (s, 1H), 5.91 (s, 1H), 4.60–4.30 (m, 2H), 4.21–4.10 (m, 2H), 3.95–3.93 (m, 1H), 3.80–3.76 (m, 1H), 3.26–3.24 (m, 1H), 3.02–2.97 (m, 4H), 2.12–1.80 (m, 3H), 1.85–1.75 (m, 3H).

Ethyl 2-(4-(6-(Benzod[[1,3]dioxol-5-yl)-1,4-dioxo-3,4,6,7,12,12a-hexahdropyrazino[1',2':1,6]pyrido[3,4-b]indol-2(1H)-yl)piperidin-1-yl)pyrimidine-5-carboxylate (37b). To a solution of compound 36a (0.5 g, 1.09 mmol) in CH₃CN (10 mL) was added ethyl 2-chloropyrimidine-5-carboxylate (0.41 g, 2.18 mmol), K₂CO₃ (0.45 g, 3.27 mmol), and KI (0.036 g, 0.22 mmol), and the reaction mixture was stirred at room temperature for 5 h. Then, the mixture was concentrated and extracted with EtOAc. The combined organic layers were washed with brine, dried over anhydrous Na₂SO₄, filtered, and concentrated to give the crude product which was purified by column chromatography to afford pure compound 37b (0.6 g, 90%) as a yellow solid. ESI-MS *m/z* 609 [M + H]⁺ calcd for C₃₃H₃₂N₆O₆. ¹H NMR (CDCl₃, 400 MHz): δ 8.83 (s, 2H), 7.86 (s, 1H), 7.63–7.61 (m, 1H), 7.29–7.26 (m, 1H), 7.19–7.16 (m, 2H), 6.80–6.81 (m, 1H), 6.70–6.67 (m, 2H), 6.17 (s, 1H), 5.87 (d, *J* = 9.2 Hz, 2H), 5.08–5.05 (m, 2H), 4.81–4.75 (m, 1H), 4.36–4.28 (m, 3H), 3.91–3.88 (m, 2H), 3.73–3.72 (m, 1H), 3.27–3.23 (m, 1H), 3.05–2.99 (m, 2H), 1.85–

1.80 (m, 1H), 1.80–1.77 (m, 1H), 1.62–1.59 (m, 2H), 1.38–1.36 (m, 3H).

2-(4-(6-(Benzod[[1,3]dioxol-5-yl)-1,4-dioxo-3,4,6,7,12,12a-hexahdropyrazino[1',2':1,6]pyrido[3,4-b]indol-2(1H)-yl)piperidin-1-yl)pyrimidine-5-carboxylic acid (38b). To a solution of compound 37b (0.4 g, 0.66 mmol) in THF/H₂O (2:1, 30 mL) was added LiOH·H₂O (0.22 g, 5 mmol), and the reaction mixture was stirred at room temperature overnight. Then, the mixture was diluted with EtOAc and washed with 2.0 M HCl aqueous solution. The organic layer was dried over anhydrous Na₂SO₄, filtered, and concentrated to give compound 38b (0.2 g, 51%) as a yellow solid. ESI-MS *m/z* 581 [M + H]⁺ calcd for C₃₁H₂₈N₆O₆. This intermediate was used in the next step without further characterization.

2-(4-(6-(Benzod[[1,3]dioxol-5-yl)-1,4-dioxo-3,4,6,7,12,12a-hexahdropyrazino[1',2':1,6]pyrido[3,4-b]indol-2(1H)-yl)piperidin-1-yl)-N-(tetrahydro-2H-pyran-2-yl)oxy)pyrimidine-5-carboxamide (39b). To a solution of compound 38b (260 mg, 0.45 mmol) in DMF (10 mL) was added EDC·HCl (173 mg, 0.9 mmol), HOBr (122 mg, 0.9 mmol), THPONH₂ (63 mg, 0.54 mmol), and NMM (136 mg, 1.35 mmol), and the mixture was stirred at 30 °C overnight. Then, the reaction mixture was diluted with EtOAc, washed with brine, dried over anhydrous Na₂SO₄, filtered, and purified by column chromatography to give the desired compound 39b (250 mg, 82%) as a pale yellow solid. ESI-MS *m/z* 680 [M + H]⁺ calcd for C₃₆H₃₇N₇O₇. This intermediate was used in the next step without further characterization.

2-(4-(6-(Benzod[[1,3]dioxol-5-yl)-1,4-dioxo-3,4,6,7,12,12a-hexahdropyrazino[1',2':1,6]pyrido[3,4-b]indol-2(1H)-yl)piperidin-1-yl)-N-hydroxypyrimidine-5-carboxamide (40b). A solution of compound 39b (125 mg, 0.18 mmol) in HCl/1,4-dioxane (3.0 M, 10 mL) was stirred at room temperature overnight. Then, the reaction mixture was concentrated and purified by preparative HPLC (method 2 described in the Supporting Information) to give compound 40a (22.6 mg, 21%) as a pale yellow solid. ESI-MS *m/z* 596.3 [M + H]⁺ calcd for C₃₁H₂₉N₇O₆. ¹H NMR (DMSO, 400 MHz): δ 11.04 (s, 2H), 8.67 (s, 2H), 7.52–7.50 (m, 1H), 7.32–7.30 (m, 1H), 7.10–7.08 (m, 1H), 7.04–7.02 (m, 1H), 6.88–6.87 (m, 1H), 6.81–6.76 (m, 2H), 6.63–6.61 (m, 1H), 6.01 (s, 2H), 4.87–4.81 (m, 2H), 4.53–4.41 (m, 1H), 4.15–4.12 (m, 2H), 4.00–3.96 (m, 1H), 3.29–3.25 (m, 1H), 3.02–2.95 (m, 3H), 1.72–1.66 (m, 4H).

Ethyl (E)-3-(4-(4-(6-(Benzod[[1,3]dioxol-5-yl)-1,4-dioxo-3,4,6,7,12,12a-hexahdropyrazino[1',2':1,6]pyrido[3,4-b]indol-2(1H)-yl)piperidin-1-yl)methyl)phenyl)acrylate (37c). To a solution of compound 36a (1 g, 2.18 mmol) in CH₃CN (10 mL) was added ethyl (E)-3-[4-(methylsulfonyloxy)methyl]phenylprop-2-enate (0.55 g, 1.9 mmol) and K₂CO₃ (0.55 g, 4 mmol), and the reaction mixture was stirred at room temperature for 5 h. Then, the mixture was concentrated and extracted with EtOAc. The combined organic layers were washed with brine, dried over anhydrous Na₂SO₄, filtered, and concentrated to give the crude product which was purified by column chromatography to afford compound 37c (0.3 g, 21%) as a yellow solid. ESI-MS *m/z* 647 [M + H]⁺ calcd for C₃₈H₃₈N₄O₆. This intermediate was used in the next step without further characterization.

(E)-3-(4-(4-(6-(Benzod[[1,3]dioxol-5-yl)-1,4-dioxo-3,4,6,7,12,12a-hexahdropyrazino[1',2':1,6]pyrido[3,4-b]indol-2(1H)-yl)piperidin-1-yl)methyl)phenyl)acrylic acid (38c). To a solution of compound 37c (50 mg, 0.08 mmol) in THF/H₂O (3:1, 8 mL) was added LiOH·H₂O (32 mg, 0.8 mmol) and the reaction mixture was stirred at room temperature overnight. Then, the mixture was diluted with EtOAc and washed with 2.0 M HCl aqueous solution. The organic layer was dried over anhydrous Na₂SO₄, filtered, and concentrated to give compound 38c (40 mg, 81%) as a yellow solid. ESI-MS *m/z* 619 [M + H]⁺ calcd for C₃₆H₃₄N₄O₆. This intermediate was used in the next step without further characterization.

(E)-3-(4-(4-(6-(Benzod[[1,3]dioxol-5-yl)-1,4-dioxo-3,4,6,7,12,12a-hexahdropyrazino[1',2':1,6]pyrido[3,4-b]indol-2(1H)-yl)piperidin-1-yl)methyl)phenyl)-N-((tetrahydro-2H-pyran-2-yl)oxy)acrylamide (39c). To a solution of compound 38c (40 mg, 0.065 mmol) in DMF (5 mL) was added EDC·HCl (25 mg, 0.13 mmol), HOBr (17.6 mg, 0.13 mmol), THPONH₂ (7.6 mg, 0.065 mmol), and NMM (19.6 mg, 0.195 mmol), and the mixture was stirred at 30 °C overnight. Then, the mixture was diluted with EtOAc

and the organic layer was washed with brine, dried over anhydrous Na_2SO_4 , filtered and concentrated to give compound **39c** (50 mg, 99% crude) as a pale yellow solid. ESI-MS m/z 718 [$\text{M} + \text{H}$]⁺ calcd for $\text{C}_{41}\text{H}_{43}\text{N}_5\text{O}_7$. This intermediate was used in the next step without further characterization.

(E)-3-((4-(6-(*Benzod*[d][1,3]dioxol-5-yl)-1,4-dioxo-3,4,6,7,12,12*a*-hexahydropyrazino[1',2':1,6]pyrido[3,4-*b*]indol-2(1H)-yl)piperidin-1-yl)methyl)phenyl)-N-hydroxyacrylamide (**40c**). A solution of compound **39c** (50 mg, 0.069 mmol) in HCl/1,4-dioxane (3.0 M, 5 mL) was stirred at room temperature overnight. Then, the reaction mixture was concentrated and purified by preparative HPLC (method 5 described in Supporting Information) to give compound **40c** (3.7 mg, 8%) as a pale yellow solid. ESI-MS m/z 634.3 [$\text{M} + \text{H}$]⁺ calcd for $\text{C}_{36}\text{H}_{35}\text{N}_5\text{O}_6$. ¹H NMR (CD_3CN , 400 MHz): δ 9.09 (s, 1H), 7.63–7.52 (m, SH), 7.34–7.32 (m, 1H), 7.17–7.12 (m, 1H), 7.09–7.07 (m, 1H), 6.88 (s, 1H), 6.82 (s, 1H), 6.77–6.75 (m, 1H), 6.70–6.65 (m, 1H), 6.52–6.49 (m, 1H), 5.94 (s, 2H), 4.52–4.46 (m, 1H), 4.20–4.17 (m, 3H), 4.02–3.87 (m, 2H), 3.48–3.44 (m, 2H), 3.35–3.32 (m, 1H), 2.98–2.95 (m, 3H), 1.82–1.77 (m, 2H).

tert-Butyl 4-((6-(*Benzod*[d][1,3]dioxol-5-yl)-1,4-dioxo-3,4,6,7,12,12*a*-hexahydropyrazino[1',2':1,6]pyrido[3,4-*b*]indol-2(1H)-yl)methyl)piperidine-1-carboxylate (**35b**). To a solution of compound **31** (3 g, 7.0 mmol) in MeOH (30 mL) was added *tert*-butyl 4-(aminomethyl)piperidine-1-carboxylate (3.0 g, 14 mmol), and the mixture was stirred at 80 °C for 2 days. Then, the mixture was concentrated and extracted with EtOAc. The combined organic layers were washed with brine, dried over anhydrous Na_2SO_4 , filtered, and concentrated to give the crude product which was purified by column chromatography to afford compound **35b** (3.2 g, 79%) as a pale yellow solid. ESI-MS m/z 573 [$\text{M} + \text{H}$]⁺ calcd for $\text{C}_{32}\text{H}_{36}\text{N}_4\text{O}_6$. ¹H NMR (CDCl_3 , 400 MHz): δ 8.11 (s, 1H), 7.65–7.60 (m, 1H), 7.30–7.25 (m, 1H), 7.25–7.10 (m, 2H), 6.85–6.80 (m, 1H), 6.75–6.60 (m, 2H), 6.21 (s, 1H), 5.87–5.86 (m, 2H), 4.36–4.30 (m, 1H), 4.15–4.02 (m, 3H), 3.95–3.90 (m, 1H), 3.80–3.70 (m, 1H), 3.45–3.30 (m, 2H), 3.25–3.20 (m, 1H), 2.70–2.60 (m, 2H), 1.90–1.80 (m, 1H), 1.60–1.55 (m, 2H), 1.46 (s, 9H), 1.30–1.1 (m, 2H).

6-(*Benzod*[d][1,3]dioxol-5-yl)-2-(piperidin-4-ylmethyl)-2,3,6,7,12,12*a*-hexahydropyrazino[1',2':1,6]pyrido[3,4-*b*]indole-1,4-dione (**36b**). To a solution of compound **35b** (3.5 g, 6.1 mmol) in CH_2Cl_2 (30 mL) was added TFA (7 mL) and the reaction mixture was stirred at room temperature for 2 h. Then, the mixture was concentrated to give compound **36b** (2.8 g, 97%) as a yellow solid. ESI-MS m/z 473 [$\text{M} + \text{H}$]⁺ calcd for $\text{C}_{27}\text{H}_{28}\text{N}_4\text{O}_4$. This intermediate was used in the next step without further characterization.

Ethyl 2-((6-(*Benzod*[d][1,3]dioxol-5-yl)-1,4-dioxo-3,4,6,7,12,12*a*-hexahydropyrazino[1',2':1,6]pyrido[3,4-*b*]indol-2(1H)-yl)methyl)piperidin-1-yl)pyrimidine-5-carboxylate (**37d**). To a solution of compound **36b** (3.3 g, 6.99 mmol) in CH_3CN (10 mL) was added ethyl 2-chloropyrimidine-5-carboxylate (1.43 g, 7.7 mmol), K_2CO_3 (1.9 g, 13.9 mmol) and KI (0.12 g, 0.69 mmol) and the reaction mixture was stirred at room temperature for 5 h. Then, the mixture was concentrated and extracted with EtOAc. The combined organic layers were washed with brine, dried over anhydrous Na_2SO_4 , filtered, and concentrated to give the crude product which was purified by column chromatography to afford compound **37d** (2.2 g, 51%) as a yellow solid. ESI-MS m/z 623 [$\text{M} + \text{H}$]⁺ calcd for $\text{C}_{34}\text{H}_{34}\text{N}_6\text{O}_6$. This intermediate was used in the next step without further characterization.

2-((6-(*Benzod*[d][1,3]dioxol-5-yl)-1,4-dioxo-3,4,6,7,12,12*a*-hexahydropyrazino[1',2':1,6]pyrido[3,4-*b*]indol-2(1H)-yl)methyl)piperidin-1-yl)pyrimidine-5-carboxylic acid (**38d**). To a solution of compound **37d** (2 g, 3.2 mmol) in THF/ H_2O (3:2, 25 mL) was added LiOH- H_2O (1.4 g, 32 mmol), and the reaction mixture was stirred at room temperature overnight. Then, the mixture was diluted with EtOAc and washed with 2.0 M HCl aqueous solution. The organic layer was dried over anhydrous Na_2SO_4 , filtered, and concentrated to give compound **38d** (1.9 g, 99% crude) as a yellow solid. ESI-MS m/z 595 [$\text{M} + \text{H}$]⁺ calcd for $\text{C}_{32}\text{H}_{30}\text{N}_6\text{O}_6$. This intermediate was used in the next step without further characterization.

2-((6-(*Benzod*[d][1,3]dioxol-5-yl)-1,4-dioxo-3,4,6,7,12,12*a*-hexahydropyrazino[1',2':1,6]pyrido[3,4-*b*]indol-2(1H)-yl)methyl)-

piperidin-1-yl)-N-((tetrahydro-2*H*-pyran-2-yl)oxy)pyrimidine-5-carboxamide (**39d**). To a solution of compound **38d** (1 g, 1.68 mmol) in DMF (10 mL) was added EDC-HCl (640 mg, 3.3 mmol), HOBT (450 mg, 3.3 mmol), THPONH₂ (190 mg, 1.68 mmol), and NMM (500 mg, 5.0 mmol), and the mixture was stirred at 30 °C overnight. Then, the mixture was diluted with EtOAc and the organic layer was washed with brine, dried over anhydrous Na_2SO_4 , filtered, and concentrated to give compound **39d** (800 mg, 68%) as a pale yellow solid. ESI-MS m/z 694 [$\text{M} + \text{H}$]⁺ calcd for $\text{C}_{37}\text{H}_{39}\text{N}_7\text{O}_7$. This intermediate was used in the next step without further characterization.

2-((6-(*Benzod*[d][1,3]dioxol-5-yl)-1,4-dioxo-3,4,6,7,12,12*a*-hexahydropyrazino[1',2':1,6]pyrido[3,4-*b*]indol-2(1H)-yl)methyl)piperidin-1-yl)pyrimidine-5-carboxamide (**40d**). A solution of compound **39d** (800 mg, 1.2 mmol) in HCl/1,4-dioxane (1.0 M, 10 mL) was stirred at room temperature overnight. Then, the mixture was concentrated and purified by preparative HPLC (method 3 described in Supporting Information) to give **40d** (204 mg, 27%) as a pale yellow solid. ESI-MS m/z 610.3 [$\text{M} + \text{H}$]⁺ calcd for $\text{C}_{32}\text{H}_{31}\text{N}_7\text{O}_6$. ¹H NMR (DMSO, 400 MHz): δ 11.03 (s, 2H), 8.62 (s, 2H), 7.52–7.50 (m, 1H), 7.30–7.28 (m, 1H), 7.08–6.99 (m, 1H), 6.85–6.84 (m, 1H), 6.80 (s, 1H), 6.74 (s, 1H), 6.60–6.58 (m, 1H), 6.00 (s, 2H), 4.67–4.64 (m, 2H), 4.32–4.28 (m, 1H), 4.08–3.99 (m, 2H), 3.45–3.40 (m, 1H), 3.26–3.23 (m, 1H), 3.01–2.89 (m, 4H), 2.10–1.90 (m, 1H), 1.72–1.66 (m, 2H), 1.10–1.05 (m, 2H).

Docking into HDAC1, HDAC2, and PDE5. Docking simulations into the crystal structure of HDAC1 (PDB entry 4BKX⁴³), HDAC2 complexed with SAHA (PDB entry 4LXZ²⁴), and PDE5 complexed with sildenafil (PDB entry 1TBF⁴⁴) were carried out with the Gold program.⁴⁵ The binding site was defined as a 20 Å sphere around the Zn atom (HDACs) and the nitrogen of Gln817 (PDE5). The PLP scoring function was used to rank docking poses, requiring a total of 100 poses per ligand. Optimization parameters were left at the “slow-accurate docking” settings. Previous validation (RMSD < 2 Å) was carried out for docking of SAHA into HDAC2 and sildenafil into PDE5.

Acetyl-Histone H3 Lysine 9 (H3K9ac) Cellular Detection Assay (AlphaLisa Technology). Briefly, 2000 cells (SH-SYSY) were plated in a poly-D-lysine- treated 384-well plate. Cells were incubated with different concentrations of SAHA and vardenafil or compound **22** during 2 h. After incubation, the medium was removed and cells were lysed, histones were extracted and histone carrying the acetylation mark was detected following the manufacturer’s instructions (PerkinElmer; cat. # AL714 A/C kit assay). Signal of acetylation mark was obtained after 18 h of dark incubation at room temperature and was normalized by the unmodified histone signal and calculated as folds over basal levels, considered as those obtained in the absence of assayed compounds.

HDACs and PDEs Enzyme Activity Assays. HDACs enzyme activities were measured with a specific fluorescence-labeled substrate (BPS Biosciences, cat. # 50037) after its deacetylation by HDACs. The fluorogenic substrate, containing an acetylated lysine side chain, can be deacetylated and then sensitized to subsequent treatment with the lysine developer, which produces a fluorophore that can be measured with a fluorescence plate reader. Human HDAC1 (GenBank Accession No. NM_004964), full length, with C-terminal His-tag and C-terminal Flag-tag, was obtained from BPS Biosciences (cat. # 50051). Human HDAC2 (GenBank Accession No. NM_001527), full length, with C-terminal His-tag was obtained from BPS Biosciences (cat. # 50002). Human HDAC3 (GenBank Accession No. NM_003883), full length, with C-terminal His-tag and human NCOR2, N-terminal GST-tag was obtained from BPS Biosciences (cat. # 50003). Human HDAC6 (GenBank Accession No. BC069243), full length with N-terminal GST tag was obtained from BPS Biosciences (cat. # 50006). A volume of 5 μL of vehicle or tested compound 10× concentrated prepared in assay buffer (BPS Biosciences, cat. # 50031) were added in black 96-well plates (final volume of 100 μL). The final percentage of DMSO was 1%. A volume of 5 μL of HDAC1 (4 μg/mL) or HDAC2 (15 μg/mL) or HDAC3 (10 μg/mL) or HDAC6 (36 μg/mL) enzyme in assay buffer was added (final HDAC1, HDAC2, HDAC3, and HDAC6 concentration of 0.4, 1.5, 0.1, and 3.6 μg/mL respectively) and the

reaction was started by the addition of 40 μL of reaction mixture containing 0.125 mg/mL BSA (final concentration of 0.1 mg/mL) and 12.5 μM of fluorogenic HDACs substrate (final concentration of 10 μM). The reaction was incubated for 30 min at 37 °C. After incubation, the reaction was stopped with 50 μL of lysine assay developer (BPS Biosciences, cat. # 50030). After incubation during 20 min at room temperature, the fluorescence of each well was measured at 355 nm excitation and 460 nm emission in a Mithras plate reader (Berthold). Positive control was obtained in the presence of the vehicle of the compounds. Negative control was obtained in the absence of HDAC enzyme activity. A best fit curve was fitted using GraphPad Prism 5 to derive the half maximal inhibitory concentration (IC_{50}) from this curve.

PDESA and PDE9A enzyme activity was measured with the HTRF cGMP assay kit from CisBio (CisBio, cat. #62GM2PEB), which determines the amount of cGMP present in the reaction. Human PDE5A1 (GenBank Accession No. NM_001083) or human PDE9A isoform b (GenBank Accession No. NM_001083), full length, with N-terminal GST tag was obtained from BPS Biosciences (cat. # 60050 or # 60090). A volume of 2.5 μL of vehicle or tested compound 4 \times concentrated prepared in assay buffer (50 mM Tris-HCl, 6 mM MgCl₂, pH 7.4) were added in 384-well plates (final volume of 20 μL). The final percentage of DMSO was 0.5%; 2.5 μL of PDESA (7 $\mu\text{g}/\text{mL}$) or of PDE9A (0.2 $\mu\text{g}/\text{mL}$) enzyme in assay buffer was added (final PDESA concentration 1.75 $\mu\text{g}/\text{mL}$ or final PDE9A concentration 0.05 $\mu\text{g}/\text{mL}$) and the reaction was started by the addition of 5 μL of substrate cGMP (4 \times concentrated) to a final concentration of 100 nM cGMP. The reaction was incubated for 30 min at 37 °C. After incubation, the reaction was stopped with 5 μL of cGMP-D2 (cGMP labeled with the dye D2) and 5 μL of Mab anti-cGMP labeled with cryptate (cGMP-cryptate). After incubation during 1 h at room temperature, the fluorescence of each well was measured at 665 nm excitation and 620 nm emission in an Envision plate reader (PerkinElmer) and the results were expressed as the 665 nm/620 nm ratio. Positive control was obtained in the presence of the vehicle of the compounds. Negative control was obtained in the absence of cGMP and labeled cGMP-D2 cyclic nucleotide. A best fit curve was fitted using GraphPad Prism 5 to derive the half maximal inhibitory concentration (IC_{50}) from this curve. PDE3A and PDE6C enzyme activity assays were carried out at BPS Bioscience (<https://bpsbioscience.com/>).

Cytotoxicity in THLE-2 Cells. Cytotoxic effects of assayed compounds were tested using the immortalized human liver cell line THLE-2 (ATCC CRL-2706), cultured in BEGM medium (Clonetics #CC-4175). Medium was completed by adding 0.7 $\mu\text{g}/\text{mL}$ phosphoethanolamine, 0.5 ng/mL epidermal growth factor, antibiotics (penicillin and streptomycin) and 10% fetal bovine serum (FBS). Cells were plated in 96-well black microplates at 10,000 cells/well and incubated at 37 °C (5% CO₂, 95% humidity) for 24 h. Test compounds were solubilized in 100% DMSO and then diluted with cell culture medium containing 10% DMSO. The final concentrations of the test compounds (1% DMSO) ranged from 0 to 100 μM in a final volume of 200 μL . After 72 h, cell viability in each well was determined by measuring the concentration of cellular adenosine triphosphate (ATP) using the VialightTM Plus Cell Proliferation/Cytotoxicity Kit as described by the manufacturer (Cambrex, East Rutherford, NJ). After addition of cell lysis buffer, test plate was incubated for 45 min at room temperature (orbital shaker). ATP monitoring solution was added and ATP concentration determined by reading luminescence using a Envision plate reader (PerkinElmer). The percentage of viable cells relative to the nondrug treated controls was determined for each well and LC₅₀ values were calculated as concentrations projected to kill 50% of the cells following a 24 or 72 h exposure.

Cytotoxicity in Neuron Glia Cells. Cytotoxic effects of assayed compounds were tested using primary cultures of mice brain embryo tissue. Cells growth in 96-well black microplates were incubated at 37 °C (5% CO₂, 95% humidity) for 5 days to permit neurons formation. After that, 100 $\mu\text{L}/\text{well}$ of medium and studied compounds was added. Test compounds were solubilized in 100% DMSO at a concentration

curve way and then diluted with cell culture medium containing 10% DMSO. The final concentrations of the test compounds (1% DMSO) ranged from 0 to 100 μM in a final volume of 200 μL . Microplates were maintained at 37 °C (5% CO₂, 95% humidity) during 3 days. Following this 72 h exposure to test compounds, cell viability in each well was determined by measuring the concentration of cellular adenosine triphosphate (ATP) using the ATP1Step Kit as described by the manufacturer (PerkinElmer). In a typical procedure, 50 μL of cell reagent is added to all wells of each test plate followed by incubation for 10 min at room temperature on an orbital shaker. ATP concentration was determined by reading chemical luminescence using the Envision plate reader (PerkinElmer). The percentage of viable cells relative to the nondrug treated controls was determined for each well and LC₅₀ values were calculated as concentrations projected to kill 50% of the cells following a 72 h exposure.

Cytotoxicity in PBMCs. Cytotoxic effects of assayed compounds were tested using peripheral blood mononuclear cells isolated following the regular density gradient centrifugation procedure with Ficol. Cells were plated in 96-well black microplates at 100 000 cells/well density with DMEM medium (containing 10% FBS and antibiotics) and were incubated at 37 °C (5% CO₂, 95% humidity) for 24 h. Test compounds were solubilized in 100% DMSO at a concentration curve way and then diluted with cell culture medium containing 10% DMSO. The final concentrations of the test compounds (1% DMSO) ranged from 0 to 100 μM in a final volume of 200 μL . Microplates were maintained at 37 °C (5% CO₂, 95% humidity) during 3 days. Following this 72 h exposure to test compounds, cell viability in each well was determined by measuring the concentration of cellular adenosine triphosphate (ATP) using the ATP1Step Kit as described by the manufacturer (PerkinElmer). In a typical procedure, 80 μL of cell reagent is added to all wells of each test plate followed by incubation for 10 min at room temperature on an orbital shaker. ATP concentration was determined by reading chemical luminescence using the Envision plate reader (PerkinElmer). The percentage of viable cells relative to the nondrug treated controls was determined for each well and LC₅₀ values were calculated as concentrations projected to kill 50% of the cells following a 72 h exposure.

PAMPA Permeability. The permeability of compounds was evaluated with the parallel artificial membrane permeation assay (PAMPA) as an *in vitro* model of passive diffusion. Donor solutions of test compounds (180 μL , 50 μM in PBS/ETOH 70:30) were added to each well of the donor plate, whose PVDF membrane was precoated with 4 μL of a 20 mg \times mL⁻¹ PBL/dodecane mixture. PBS/EtOH (180 μL) was added to each well of the PTFE acceptor plate. The donor and acceptor plates were combined together and incubated for 18 h at 20 °C without shaking. In each plate, compounds and controls were tested in duplicate. Drug concentration in the acceptor, the donor, and the reference wells was determined using the UV plate reader with 130 μL of acceptor and donor samples. Permeability rates (Pe in nm s⁻¹) were calculated with eq 1. The permeability rate of each compound is the averaged value of three independent measurements.

$$P_e = C \left(-\ln \left(1 - \frac{[\text{drug}]_{\text{acceptor}}}{[\text{drug}]_{\text{equilibrium}}} \right) \right) \times 10^7 \quad (1)$$

where $C = \frac{V_D V_A}{(V_D + V_A) \times \text{area} \times \text{time}}$; $V_D = 0.18 \text{ mL}$; $V_A = 0.18 \text{ mL}$; area = 0.32 cm²; time = 64 800 s; $D_F = 180/130$; $[\text{drug}]_{\text{equilibrium}} = ([\text{drug}]_{\text{donor}} \times V_D + [\text{drug}]_{\text{acceptor}} \times V_A)/(V_D + V_A)$; $[\text{drug}]_{\text{donor}} = (A_a/A_i \cdot D_F)_{\text{donor}}$; $[\text{drug}]_{\text{acceptor}} = (A_a/A_i \cdot D_F)_{\text{acceptor}}$; $A_{a,\text{donor}} = \text{Abs}_{\text{donor}} - \text{Abs}_{\text{vehicle}}$; $A_{a,\text{acceptor}} = \text{Abs}_{\text{acceptor}} - \text{Abs}_{\text{vehicle}}$; $A_i = \text{Abs}_{\text{withoutPBL}} - \text{Abs}_{\text{vehicle}}$.

PDE and HDAC Functional Response in Vitro. To analyze the functional activity of the different compounds we used primary neuronal cultures and human neuroblastoma SH-SY5Y cell line. Primary neuronal cultures were obtained from the hippocampus and cortex of embryonic day 16 (E16) Tg2576 mice and used at 15 days or 21 days *in vitro* (DIV).¹⁷

In Vivo Functional Response. To confirm the ability of **22** to exert a functional response in the brain, the compound (40 mg/kg, i.p.) was administered to WT mice ($n = 3$). At different times (15, 30, and 60 min), mice were sacrificed and their hippocampus was quickly dissected from the brains. Total tissue homogenates were obtained by homogenizing the hippocampus in a lysis buffer containing Tris HCl 10 mM, NaF 1 mM, NaVO₄ 0.1 mM, sodium dodecyl sulfate (SDS) 2%, and protease inhibitors. Western blot was carried out to analyze pCREB-Ser133.

Western Blot Analysis. For Western blot analysis of histones, pCREB, and tubulin, protein samples were mixed with 6× Laemmli sample buffer and resolved onto SDS-polyacrylamide gels and transferred to nitrocellulose membrane. In all cases, the membranes were blocked with 5% milk, 0.05% Tween-20 in tris-buffered saline (TBS) followed by overnight incubation with the following primary antibodies: rabbit monoclonal anti-acetylated H3 (Lys9), rabbit monoclonal anti-pCREB (Ser133), mouse monoclonal anti-actin, mouse monoclonal anti-acetylated-tubulin (1:20 000, Sigma-Aldrich, St. Louis, MO) in the corresponding buffer. Following two washes in PBS/Tween-20 or TBS/Tween-20 and one PBS or TBS alone, immunolabeled protein bands were detected by using HRP-conjugated anti-rabbit or anti-mouse antibody (1:5000, Santa Cruz Biotechnology, Santa Cruz, CA) or anti-goat (1:1500, Dako) antibody following an enhanced chemiluminescence system (ECL, GE Healthcare Bioscience, Buckinghamshire, UK), and autoradiographic exposure to Hyperfilm ECL (GE Healthcare Bioscience). Quantity One software v.4.6.3 (Bio-Rad, Hercules, CA) was used for quantification.

For Western blot analysis of APP-derived fragments, protein extracts were mixed with tricine sample buffer 1:2 (Bio-Rad) and 2% βME, and after they were boiled for 5 min. Proteins were separated in a CriterionTM Tris-Tricine 10–20% gradient precast gel (Bio-Rad, Hercules, CA) and transferred to a PVDF membrane with 0.2 μm removal rating (Hybond LFP, Amersham Biosciences, Little Chalfont, UK). For analysis of pTau, aliquots of the protein extracts were mixed with XT sample buffer plus XT reducing agent (Bio-Rad) and boiled for 5 min. Proteins were separated in a Criterion TM Bis-Tris 4–12% gradient precast gel (Bio-Rad, Hercules, CA). Membranes were blocked with 5% milk, 0.05% Tween-20 in tris-buffered saline (TBS) followed by overnight incubation with the following primary antibodies: mouse monoclonal 6E10 (amino acids 1–16 of Aβ peptide, 1:1000, Covance, San Diego, CA), mouse monoclonal anti-p-Tau AT8 (1:1000; Thermo Fisher Scientific, Rockford), mouse monoclonal anti-tau (1:5000, clone Tau46, Sigma-Aldrich, St. Louis, MO), mouse monoclonal anti-actin, mouse monoclonal anti-acetylated-tubulin (1:20 000, Sigma-Aldrich, St. Louis, MO) in the corresponding buffer.

CYP Inhibition. The inhibitory effect of compound **22** on five human cytochrome P450s (1A2, 2C9, 2C19, 2D6 and 3A4) was evaluated in human liver microsomes at Wuxi (<http://www.wuxi.com/>). Compound **22** (10 μM) and the corresponding substrates for each P450 isoform (20 μL) were incubated with 140 μL liver microsomes (0.286 mg/mL; BD Gentest) and NADPH cofactor (20 μL, 1 mM) for 10 min at 37 °C. The reaction was terminated by adding 400 μL cold stop solution (200 ng/mL tolbutamide in ACN) and samples were centrifuged at 4000 rpm for 20 min. Supernatants were analyzed by LC-MS/MS (Shimadzu LC 20-AD-API 4000), using peak area ratio of analyte/internal standard. Test compound and positive controls were tested in duplicates. The percentage of inhibition was calculated as the ratio of substrate metabolite detected in treated and nontreated wells.

Plasma Protein Binding. This study was conducted at Wuxi (<http://www.wuxi.com/>) by Equilibrium Dialysis. HT-Dialysis plate (model HTD 96 b, cat. # 1006) and the dialysis membrane (molecular weight cutoff 12–14 kDa, cat. # 1101) were purchased from HT Dialysis LLC (Gales Ferry, CT). Human plasma and CD-1 mouse plasma from Bioreclamation were thawed prior to experiment and the pH was adjusted at 7.4. Concentrations of test compounds in starting solution (before dialysis), plasma side of the membrane and buffer side of the membrane were quantified by LC-MS/MS (Shimadzu LC 20-AD-API 4000) methodologies, using peak area ratio of analyte/

internal standard. The fraction of unbound, bound and recovery were calculated.

Kinetic Solubility. This study was conducted at Wuxi (<http://www.wuxi.com/>) at pH 7.4 (50 mM phosphate buffer).

Human and Mouse Liver Microsomal Stability. The data collected are analyzed to calculate a half-life ($t_{1/2}$, min) for test compounds at a final concentration of 1 μM. A volume of 5 μL of stock solution of test compound (10 mM) were diluted in 495 μL of 1:1 Methanol/Water (final concentration of 100 μM, 50% MeOH). Then, 50 μL of this intermediate solution were diluted in 450 μL of 100 mM potassium phosphate buffer to a concentration of 10 μM (working solution, 5% MeOH). The NADPH regenerating system contains β-Nicotinamide adenine dinucleotide phosphate (Sigma, cat. # N0505), Isocitric acid (Sigma, cat. #I1252) and Isocitric dehydrogenase (Sigma, cat. #I2002) at a final concentration of 1 unit/mL at incubation. Human liver microsomes were obtained from BD Gentest (cat. #452117) and mouse liver microsomes from Xenotech (cat. #M1000), to a final concentration of 0.7 mg protein/mL. A volume of 10 μL of working solution and 80 μL of microsome solution were added to a 96-well plate and incubated for 10 min at 37 °C. The reaction was started by the addition of 10 μL of NADPH regenerating system and stopped by the addition of 300 μL of stop solution (ACN at 4 °C, including 100 ng/mL Tolbutamide and 100 ng/mL of Labetalol as internal standard) at different incubation times (0, 5, 10, 20, 30, and 60 min). Concentrations of test compound were quantified by LC-MS/MS methodologies (Shimadzu LC 20-AD/API4000) using peak area ratio of analyte/internal standard and the percent loss of parent compound was calculated under each time point to determine the half-life.

Determination of Brain to Plasma Concentration Ratio at Different Times. Compound **22** was measured in plasma and brain samples using an Acquity UPLC system (Waters, Manchester, UK) coupled to a Xevo-TQ MS triple quadrupole mass spectrometer with electrospray ionization (ESI) source. Plasma and brain samples were collected at different times (0.25, 0.5, and 1 h). Compound **22** was injected (40 mg/kg, i.p.) to mice ($n = 3$ per time point). Three control mice were sacrificed 30 min after the administration of vehicle solution. Compound solutions were prepared by dissolving the solid in DMSO and this solution was diluted with a mixture of Tween 20 and 0.9% NaCl, up to a final composition of 1:1:8 (v:v:v, DMSO/Tween 20/saline). Blood was collected at the different time points in EDTA-coated tubes and centrifuged at 2500 rpm for 5 min at 4 °C to obtain the plasma. The brain was removed following whole body perfusion with saline. All plasma and brain samples were stored at –80 °C until further analysis. Chromatographic separation was performed by gradient elution at 0.45 mL/min using a XSelect CSH C18 column (50 × 2.1 mm, 2.5 um; Waters). The mobile phase consisted of A: water with 0.1% formic acid, B: methanol with 0.1% formic acid. The autosampler temperature was set at 10 °C and column temperature at 40 °C. For detection and quantification, the electrospray ionization operated in the positive mode was set up for multiple reaction monitoring (MRM). The collision gas used was ultrapure argon at a flow rate of 0.15 mL min⁻¹.

At the time of analysis, frozen plasma samples were thawed at room temperature, vortex-mixed thoroughly and 25 μL were subjected to the sample preparation procedure described below. Brain samples were thawed unassisted at room temperature, homogenized using a Branson 250 ultrasonic probe sonicator (Branson, Danbury, CT), and 75 mg of the homogenate was subjected to the sample preparation procedure described below. Quantification was achieved by external calibration using matrix-matched standards. Concentrations were calculated using a weighted least-squares linear regression ($W = 1/x$). Calibration standards were prepared by adding the appropriate volume of diluted solutions of the compound (made in a mixture of methanol and water, 50:50, v:v) to either aliquots of 25 μL of blank plasma or 75 mg of the blank brain homogenate. The calibration standard and sample preparation is as follows: 2% formic acid in acetonitrile was added to precipitate the proteins. The mixture was then vortex-mixed for 5 min and centrifuged at 13200 rpm for 10 min at 4 °C. The resulting supernatants were transferred to an Ostro plate (Waters, Manchester,

UK), designed to remove phospholipids. The resulting eluents were evaporated at 37 °C under a stream of nitrogen. Plasma and brain residues were dissolved in 100 and 120 µL, respectively, of a mixture of methanol and water with 0.1% formic acid (25:75, v:v). A 5 µL aliquot of the resulting solution was injected into the LC-MS/MS system for analysis.

■ ASSOCIATED CONTENT

Supporting Information

The Supporting Information is available free of charge on the ACS Publications website at DOI: [10.1021/acscchemneuro.6b00370](https://doi.org/10.1021/acscchemneuro.6b00370).

Details about purification methods, SFC methods, synthesis of intermediates, purities, heat map with pIC₅₀ and pLC₅₀ values for sildenafil and vardenafil-based compounds as well as biochemical activities as pIC₅₀ values; functional response (AcH3K9) achieved by 22 (as dose-response curve) ([PDF](#))

■ AUTHOR INFORMATION

Corresponding Author

*Phone: +34 948 19 47 00, ext 2044. E-mail: julenoyerzabal@unav.es.

ORCID

Julen Oyarzabal: [0000-0003-1941-7255](https://orcid.org/0000-0003-1941-7255)

Author Contributions

[†]J.A.S.-A., O.R., M.C.-T., A.G.-O., and J.O. contributed equally to this work.

Notes

The authors declare no competing financial interest.

■ ACKNOWLEDGMENTS

We thank the Foundation for Applied Medical Research (FIMA), University of Navarra (Pamplona, Spain), Asociación de Amigos of University of Navarra as well as to Fundación Fuentes Dutor for financial support. This work has been partially supported through Ministerio de Economía y Competitividad (FIS PI12/00710). This work was supported by grants from FIS projects (11/02861 and 14/01244).

■ ABBREVIATIONS

AcOH, acetic acid; ADME, absorption, distribution, metabolism and excretion; BOC, *tert*-butoxycarbonyl; BOP, (benzotriazol-1-yl)oxytris(dimethylamino)phosphonium hexafluorophosphate; cAMP, cyclic adenosine monophosphate; cGMP, cyclic guanosine monophosphate; CREB, cAMP response element-binding protein; DCC, *N,N'*-dicyclohexylcarbodiimide; DIEA, diethanolamine; DMAP, 4-(*N,N*-dimethylamino)-pyridine; DMF, dimethylformamide; DMSO, dimethyl sulfoxide; EDC·HCl, 1-ethyl-3-(3-(dimethylamino)propyl)-carbodiimide hydrochloride; ESI-MS, electrospray ionization mass spectrometry; Et₃N, triethylamine; EtOAc, ethyl acetate; EtOH, ethanol; FDA, Food and Drug Administration; HDAC, histone deacetylase; HOBt, hydroxybenzotriazole; HPLC, high-performance liquid chromatography; LCMS, liquid chromatography-mass spectrometry; MeOH, methanol; MW, microwave; NIS, *N*-iodosuccinimide; NMM, *N*-methylmorpholine; NMR, nuclear magnetic resonance; PAMPA, parallel artificial membrane permeability assay; PDE, phosphodiesterase; PDES, phosphodiesterase-5; PKA, Protein Kinase A; Rt, retention time; rt, room temperature; TFA, trifluoroacetic acid; THF, tetrahydrofuran; THP, tetrahydropyranyl; THPONH₂, *N*-

(tetrahydro-2*H*-pyran-2-yl)amine; TLC, thin layer chromatography; xantphos, 4,5-bis(diphenylphosphino)-9,9-dimethyl-xanthene

■ REFERENCES

- García-Osta, A., Cuadrado-Tejedor, M., García-Barroso, C., Oyarzábal, J., and Franco, R. (2012) Phosphodiesterases as therapeutic targets for Alzheimer's disease. *ACS Chem. Neurosci.* 3, 832–44.
- Umar, T., and Hoda, N. ul. (2015) Selective inhibitors of phosphodiesterases: therapeutic promise for neurodegenerative disorders. *MedChemComm* 6, 2063–2080.
- Heckman, P. R. A., Wouters, C., and Prickaerts, J. (2015) Phosphodiesterase inhibitors as a target for cognition enhancement in aging and Alzheimer's disease: a translational overview. *Curr. Pharm. Des.* 21, 317–31.
- García-Barroso, C., Ugarte, A., Martínez, M., Rico, A. J., Lanciego, J. L., Franco, R., Oyarzábal, J., Cuadrado-Tejedor, M., and García-Osta, A. (2014) Phosphodiesterase inhibition in cognitive decline. *J. Alzheimer's Dis.* 42 (Suppl 4), S561–73.
- Cuadrado-Tejedor, M., Oyarzábal, J., Lucas, M. P., Franco, R., and García-Osta, A. (2013) Epigenetic drugs in Alzheimer's disease. *Biomol. Concepts* 4, 433–45.
- Cacabelos, R., and Torrellas, C. (2014) Epigenetic drug discovery for Alzheimer's disease. *Expert Opin. Drug Discovery* 9, 1059–86.
- Cuadrado-Tejedor, M., Hervias, I., Ricobaraza, A., Puerta, E., Pérez-Roldán, J. M., García-Barroso, C., Franco, R., Aguirre, N., and García-Osta, A. (2011) Sildenafil restores cognitive function without affecting β-amyloid burden in a mouse model of Alzheimer's disease. *Br. J. Pharmacol.* 164, 2029–41.
- García-Barroso, C., Ricobaraza, A., Pascual-Lucas, M., Unceta, N., Rico, A. J., Goicolea, M. A., Sallés, J., Lanciego, J. L., Oyarzábal, J., Franco, R., Cuadrado-Tejedor, M., and García-Osta, A. (2013) Tadalafil crosses the blood-brain barrier and reverses cognitive dysfunction in a mouse model of AD. *Neuropharmacology* 64, 114–23.
- Reneerkens, O. A. H., Rutten, K., Akkerman, S., Blokland, A., Shaffer, C. L., Menniti, F. S., Steinbusch, H. W. M., and Prickaerts, J. (2012) Phosphodiesterase type 5 (PDE5) inhibition improves object recognition memory: indications for central and peripheral mechanisms. *Neurobiol. Learn. Mem.* 97, 370–9.
- Tully, T. (1997) Regulation of gene expression and its role in long-term memory and synaptic plasticity. *Proc. Natl. Acad. Sci. U. S. A.* 94, 4239–41.
- Puzzo, D., Vitolo, O., Trinchese, F., Jacob, J. P., Palmeri, A., and Arancio, O. (2005) Amyloid-beta peptide inhibits activation of the nitric oxide/cGMP/cAMP-responsive element-binding protein pathway during hippocampal synaptic plasticity. *J. Neurosci.* 25, 6887–97.
- Konsoula, Z., and Barile, F. A. (2012) Epigenetic histone acetylation and deacetylation mechanisms in experimental models of neurodegenerative disorders. *J. Pharmacol. Toxicol. Methods* 66, 215–20.
- Gräff, J., and Tsai, L.-H. (2013) The potential of HDAC inhibitors as cognitive enhancers. *Annu. Rev. Pharmacol. Toxicol.* 53, 311–30.
- Benito, E., Urbanke, H., Ramachandran, B., Barth, J., Halder, R., Awasthi, A., Jain, G., Caperce, V., Burkhardt, S., Navarro-Sala, M., Nagarajan, S., Schütz, A.-L., Johnsen, S. A., Bonn, S., Lührmann, R., Dean, C., and Fischer, A. (2015) HDAC inhibitor-dependent transcriptome and memory reinstatement in cognitive decline models. *J. Clin. Invest.* 125, 3572–84.
- Ricobaraza, A., Cuadrado-Tejedor, M., Pérez-Mediavilla, A., Frechilla, D., Del Río, J., and García-Osta, A. (2009) Phenylbutyrate ameliorates cognitive deficit and reduces tau pathology in an Alzheimer's disease mouse model. *Neuropsychopharmacology* 34, 1721–32.
- Cuadrado-Tejedor, M., García-Barroso, C., Sanzhez-Arias, J., Mederos, S., Rabal, O., Ugarte, A., Franco, R., Pascual-Lucas, M., Segura, V., Perea, G., Oyarzábal, J., and García-Osta, A. (2015) Concomitant histone deacetylase and phosphodiesterase 5 inhibition

- synergistically prevents the disruption in synaptic plasticity and it reverses cognitive impairment in a mouse model of Alzheimer's disease. *Clin. Epigenet.* 7, 108.
- (17) Cuadrado-Tejedor, M., García-Barroso, C., Sánchez-Arias, J. A., Rabal, O., Mederos, S., Ugarte, A., Franco, R., Segura, V., Perea, G., Oyarzabal, J., and García-Osta, A. (2017) A first-in-class small-molecule that acts as a dual inhibitor of HDAC and PDES, and that rescues hippocampal synaptic impairment in Alzheimer's disease mice. *Neuropsychopharmacology* 42, S24.
- (18) Rabal, O., Sánchez-Arias, J. A., Cuadrado-Tejedor, M., de Miguel, I., Pérez-González, M., García-Barroso, C., Ugarte, A., Estella-Hermoso de Mendoza, A., Sáez, E., Espelosin, M., Ursua, S., Haizhong, T., Wei, W., Musheng, X., García-Osta, A., and Oyarzabal, J. (2016) Design, Synthesis, and Biological Evaluation of First-in-Class Dual Acting Histone Deacetylases (HDACs) and Phosphodiesterase 5 (PDES) Inhibitors for the Treatment of Alzheimer's Disease. *J. Med. Chem.* 59, 8967–9004.
- (19) Saluste, G., Albaran, M. I., Alvarez, R. M., Rabal, O., Ortega, M. A., Blanco, C., Kurz, G., Salgado, A., Pevarello, P., Bischoff, J. R., Pastor, J., and Oyarzabal, J. (2012) Fragment-Hopping-Based Discovery of a Novel Chemical Series of Proto-Oncogene PIM-1 Kinase Inhibitors. *PLoS One* 7, e45964.
- (20) Oyarzabal, J., Howe, T., Alcazar, J., Andrés, J. I., Alvarez, R. M., Dautzenberg, F., Iturriño, L., Martínez, S., and Van der Linden, I. (2009) Novel approach for chemotype hopping based on annotated databases of chemically feasible fragments and a prospective case study: new melanin concentrating hormone antagonists. *J. Med. Chem.* 52, 2076–89.
- (21) Bischoff, E. (2004) Potency, selectivity, and consequences of nonselectivity of PDE inhibition. *Int. J. Impotence Res.* 16 (Suppl 1), S11–4.
- (22) Atadja, P. (2009) Development of the pan-DAC inhibitor panobinostat (LBH589): successes and challenges. *Cancer Lett.* 280, 233–41.
- (23) Arts, J., King, P., Mariën, A., Floren, W., Beliën, A., Janssen, L., Pilatte, I., Roux, B., Decrane, L., Gilissen, R., Hickson, I., Vreys, V., Cox, E., Bol, K., Talloen, W., Goris, I., Andries, L., Du Jardin, M., Janicot, M., Page, M., van Emelen, K., and Angibaud, P. (2009) JNJ-26481585, a novel "second-generation" oral histone deacetylase inhibitor, shows broad-spectrum preclinical antitumoral activity. *Clin. Cancer Res.* 15, 6841–51.
- (24) Lauffer, B. E. L., Mintzer, R., Fong, R., Mukund, S., Tam, C., Zilberleyb, I., Flicke, B., Ritscher, A., Fedorowicz, G., Vallero, R., Ortwine, D. F., Gunzner, J., Modrusan, Z., Neumann, L., Koth, C. M., Lupardus, P. J., Kaminker, J. S., Heise, C. E., and Steiner, P. (2013) Histone deacetylase (HDAC) inhibitor kinetic rate constants correlate with cellular histone acetylation but not transcription and cell viability. *J. Biol. Chem.* 288, 26926–43.
- (25) Wang, H., Ye, M., Robinson, H., Francis, S. H., and Ke, H. (2008) Conformational variations of both phosphodiesterase-5 and inhibitors provide the structural basis for the physiological effects of vardenafil and sildenafil. *Mol. Pharmacol.* 73, 104–10.
- (26) Kim, D., Frank, C. L., Dobbin, M. M., Tsunemoto, R. K., Tu, W., Peng, P. L., Guan, J.-S., Lee, B.-H., Moy, L. Y., Giusti, P., Broodie, N., Mazitschek, R., Delalle, I., Haggarty, S. J., Neve, R. L., Lu, Y., and Tsai, L.-H. (2008) Dereulation of HDAC1 by p25/Cdk5 in Neurotoxicity. *Neuron* 60, 803–817.
- (27) Guan, J.-S., Haggarty, S. J., Giacometti, E., Dannenberg, J.-H., Joseph, N., Gao, J., Nieland, T. J. F., Zhou, Y., Wang, X., Mazitschek, R., Bradner, J. E., DePinho, R. A., Jaenisch, R., and Tsai, L.-H. (2009) HDAC2 negatively regulates memory formation and synaptic plasticity. *Nature* 459, 55–60.
- (28) Gräff, J., Rei, D., Guan, J.-S., Wang, W.-Y., Seo, J., Hennig, K. M., Nieland, T. J. F., Fass, D. M., Kao, P. F., Kahn, M., Su, S. C., Samiei, A., Joseph, N., Haggarty, S. J., Delalle, I., and Tsai, L.-H. (2012) An epigenetic blockade of cognitive functions in the neurodegenerating brain. *Nature* 483, 222–6.
- (29) Selenica, M.-L., Benner, L., Housley, S. B., Manchec, B., Lee, D. C., Nash, K. R., Kalin, J., Bergman, J. A., Kozikowski, A., Gordon, M. N., and Morgan, D. (2014) Histone deacetylase 6 inhibition improves memory and reduces total tau levels in a mouse model of tau deposition. *Alzheimer's Res. Ther.* 6, 12.
- (30) Xiong, Y., Zhao, K., Wu, J., Xu, Z., Jin, S., and Zhang, Y. Q. (2013) HDAC6 mutations rescue human tau-induced microtubule defects in Drosophila. *Proc. Natl. Acad. Sci. U. S. A.* 110, 4604–9.
- (31) Sung, Y. M., Lee, T., Yoon, H., DiBattista, A. M., Song, J. M., Sohn, Y., Moffat, E. I., Turner, R. S., Jung, M., Kim, J., and Hoe, H.-S. (2013) Mercaptoacetamide-based class II HDAC inhibitor lowers $\text{A}\beta$ levels and improves learning and memory in a mouse model of Alzheimer's disease. *Exp. Neurol.* 239, 192–201.
- (32) Zhang, L., Liu, C., Wu, J., Tao, J.-J., Sui, X.-L., Yao, Z.-G., Xu, Y.-F., Huang, L., Zhu, H., Sheng, S.-L., and Qin, C. (2014) Tubastatin A/ACY-1215 improves cognition in Alzheimer's disease transgenic mice. *J. Alzheimer's Dis.* 41, 1193–205.
- (33) McQuown, S. C., Barrett, R. M., Matheos, D. P., Post, R. J., Rogge, G. A., Alenghat, T., Mullican, S. E., Jones, S., Rusche, J. R., Lazar, M. A., and Wood, M. A. (2011) HDAC3 is a critical negative regulator of long-term memory formation. *J. Neurosci.* 31, 764–74.
- (34) Angibaud, P., Van Emelen, K., Decrane, L., van Brandt, S., Ten Holte, P., Pilatte, I., Roux, B., Poncelet, V., Speybrouck, D., Queguiner, L., Gaurrand, S., Mariën, A., Floren, W., Janssen, L., Verdonck, M., van Dun, J., van Gompel, J., Gilissen, R., Mackie, C., Du Jardin, M., Peeters, J., Noppe, M., Van Hijfte, L., Freyne, E., Page, M., Janicot, M., and Arts, J. (2010) Identification of a series of substituted 2-piperazinyl-5-pyrimidylhydroxamic acids as potent histone deacetylase inhibitors. *Bioorg. Med. Chem. Lett.* 20, 294–8.
- (35) Patel, Y., Gillet, V. J., Howe, T., Pastor, J., Oyarzabal, J., and Willett, P. (2008) Assessment of additive/nonadditive effects in structure-activity relationships: implications for iterative drug design. *J. Med. Chem.* 51, 7552–62.
- (36) Beca, S., Ahmad, F., Shen, W., Liu, J., Makary, S., Polidovitch, N., Sun, J., Hockman, S., Chung, Y. W., Movsesian, M., Murphy, E., Manganiello, V., and Backx, P. H. (2013) Phosphodiesterase type 3A regulates basal myocardial contractility through interacting with sarcoplasmic reticulum calcium ATPase type 2a signaling complexes in mouse heart. *Circ. Res.* 112, 289–97.
- (37) Card, G. L., England, B. P., Suzuki, Y., Fong, D., Powell, B., Lee, B., Luu, C., Tabrizizad, M., Gillette, S., Ibrahim, P. N., Artis, D. R., Bollag, G., Milburn, M. V., Kim, S.-H., Schlessinger, J., and Zhang, K. Y. J. (2004) Structural basis for the activity of drugs that inhibit phosphodiesterases. *Structure* 12, 2233–47.
- (38) Beghyn, T., Hounsou, C., and Deprez, B. P. (2007) PDES inhibitors: An original access to novel potent arylated analogues of tadalafil. *Bioorg. Med. Chem. Lett.* 17, 789–92.
- (39) Daugan, A., Grondin, P., Ruault, C., Le Monnier de Gouville, A.-C., Coste, H., Linget, J. M., Kirillovsky, J., Hyafil, F., and Labaudinière, R. (2003) The discovery of tadalafil: a novel and highly selective PDES inhibitor. 2:2,3,6,7,12,12a-hexahydropyrazino[1',2':1,6]pyrido[3,4-b]indole-1,4-dione analogues. *J. Med. Chem.* 46, 4533–42.
- (40) Huang, S. A., and Lie, J. D. (2013) Phosphodiesterase-5 (PDES) Inhibitors In the Management of Erectile Dysfunction. *P T* 38, 407–19.
- (41) Oyarzabal, J., Pastor, J., and Howe, T. J. (2009) Optimizing the performance of in silico ADMET general models according to local requirements: MARS approach. solubility estimations as case study. *J. Chem. Inf. Model.* 49, 2837–50.
- (42) Rabal, O., Amr, F. I., and Oyarzabal, J. (2015) Novel Scaffold FingerPrint (SFP): applications in scaffold hopping and scaffold-based selection of diverse compounds. *J. Chem. Inf. Model.* 55, 1–18.
- (43) Millard, C. J., Watson, P. J., Celardo, I., Gordiyenko, Y., Cowley, S. M., Robinson, C. V., Fairall, L., and Schwabe, J. W. R. (2013) Class I HDACs share a common mechanism of regulation by inositol phosphates. *Mol. Cell* 51, 57–67.
- (44) Zhang, K. Y. J., Card, G. L., Suzuki, Y., Artis, D. R., Fong, D., Gillette, S., Hsieh, D., Neiman, J., West, B. L., Zhang, C., Milburn, M. V., Kim, S.-H., Schlessinger, J., and Bollag, G. (2004) A glutamine switch mechanism for nucleotide selectivity by phosphodiesterases. *Mol. Cell* 15, 279–86.

- (45) Jones, G., Willett, P., and Glen, R. C. (1995) Molecular recognition of receptor sites using a genetic algorithm with a description of desolvation. *J. Mol. Biol.* 245, 43–53.